AD-A051 726 AERONAUTICAL RESEARCH LABS MELBOURNE (AUSTRALIA) F/G 13/5
STRESS ANALYSIS OF A LUG LOADED BY A PIN, (U)
JUL 77 R J CALLINAN
UNCLASSIFIED ARL-STRUC NOTE 439 NL

1 OF 1
AD
A051726

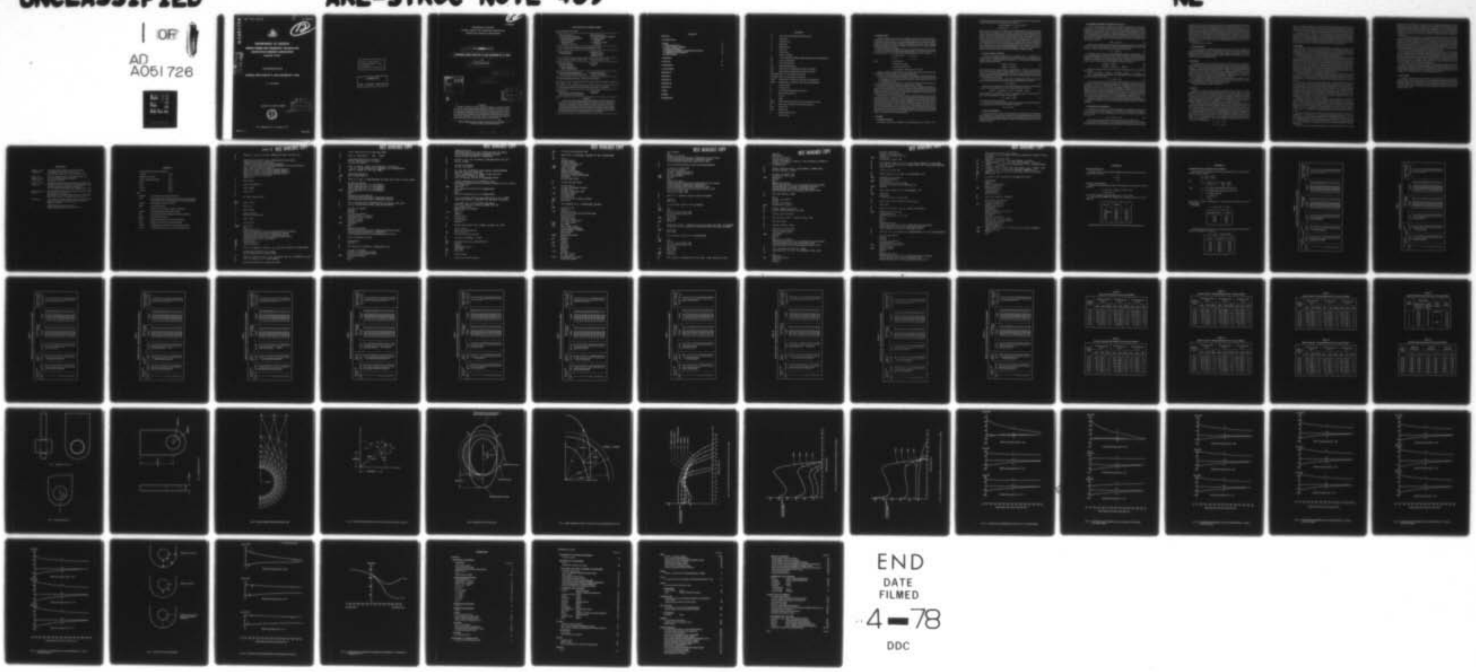

END
DATE
FILMED
4 – 78
DDC

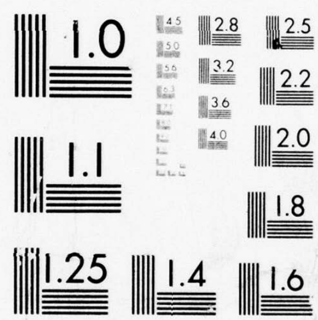
1.0
4.5
5.0
5.6
2.8
3.2
3.6
4.0
2.5
2.2
2.0
1.1
1.8
1.25
1.4
1.6

AD A051726

AD NO.
DDC FILE COPY

ARL / Struc. Note 439

AR -000-842

12

DEPARTMENT OF DEFENCE

DEFENCE SCIENCE AND TECHNOLOGY ORGANISATION

AERONAUTICAL RESEARCH LABORATORIES

MELBOURNE, VICTORIA

STRUCTURES NOTE 439

STRESS ANALYSIS OF A LUG LOADED BY A PIN

R. J. CALLINAN

Approved for Public Release

COPY No 12

July 1977

AR-000-842

DEPARTMENT OF DEFENCE

DEFENCE SCIENCE AND TECHNOLOGY ORGANISATION

AERONAUTICAL RESEARCH LABORATORIES

14 ARL-STRUC[redacted] NOTE 439

6 **STRESS ANALYSIS OF A LUG LOADED BY A PIN**

by

10 Richard R. J. CALLINAN

11 Jul 77

12 58p.

SUMMARY

A method is described which gives a refined stress analysis of a flexible lug loaded by a rigid pin. Using the finite element approach the flexibility of the lug is assessed; the contact pressure distribution is then determined by an iterative procedure which allows for compatibility of displacement between pin and lug. Having found the contact pressure the stress distribution throughout the lug is determined by a routine finite element analysis. This method is applicable to cases of neat, clearance or interference fit pins. Numerical results for neat fit pins show reasonable agreement with some test data.

POSTAL ADDRESS: Chief Superintendent, Aeronautical Research Laboratories, Box 4331, P.O., Melbourne, Victoria, 3001, Australia.

DOCUMENT DATA CONTROL SHEET

Security classification of this page

---

1. Document Numbers
   (a) AR Number: AR-000-842
   (b) Document Series and Number: Structures Note 439
   (c) Report Number: ARL/Struc.-Note-439

2. Security Classification
   (a) Complete document: Unclassified
   (b) Title in isolation: Unclassified
   (c) Summary in isolation: Unclassified

---

3. Title: STRESS ANALYSIS OF A LUG LOADED BY A PIN

---

4. Personal Author(s):
   Callinan, Richard J.

5. Document Date:
   Written June, 1977
   Published July 1977

---

6. Type of Report and Period Covered: Note

7. Corporate Author(s): ARL

---

8. Reference Numbers
   (a) Task: DST 76/152
   (b) Sponsoring Agency: Dept. of Defence (DST)

9. Cost Code:
   21 6901

---

10. Inprint (Publishing establishment):
    Aeronautical Research Laboratories Melb.

11. Computer Program(s)
    (Title(s) and language (s)):

---

12. Document Release Limitations: Approved for Public Release

12-0. Overseas: No.		P.R.	1	A		B		C		D		E	

13. Announcement Limitations (of the information on this page): No limitation

---

14. Descriptors:
    Stress analysis, Lugs, Flexibility, Pins, Stress concentration, Contact pressure

15. Cosati Codes:
    1402, 2012

16.

ABSTRACT

A method is described which gives a refined stress analysis of a flexible lug loaded by a rigid pin. Using the finite element approach the flexibility of the lug is assessed; the contact pressure distribution is then determined by an iterative procedure which allows for compatibility of displacement between pin and lug. Having found the contact pressure the stress distribution throughout the lug is determined by a routine finite element analysis. This method is applicable to cases of neat, clearance or interference fit pins. Numerical results for neat fit pins show reasonable agreement with some test data.

CONTENTS

NOTATION

$\{\delta_R\}$	Vector of radial displacements at boundary nodes
ϵ_R	Radial strain
ϵ_T	Tangential strain
σ_R	Radial stress
σ_T	Tangential stress
σ_{RT}	Shear stress
ν	Poisson's ratio
θ	Angular co-ordinate
$[A]$	Matrix of Influence Coefficients relating radial loads to radial displacements
$\{P_R\}$	A vector of radial loads
$\{P\}$	Initial load distribution
$\{P_M\}$	Modified load distribution
$[XA]$	Matrix relating X displacements of nodes to radial loads
$[YA]$	Matrix relating Y displacements of nodes to radial loads
$\{XCOORD\}$	Matrix of X Co-ordinates of node points
$\{YCOORD\}$	Matrix of Y Co-ordinates of node points
$DISPX_i$	Displacement in X direction at node i due to load distribution
$DISPY_i$	Displacement in Y direction at node i due to load distribution
E	Young's modulus
F	Fit of pin in lug
ICL	Node number defining extent of contact arc
K	Stress concentration factor
P	Pin load
R	Radius
$RDIS_{ij}$	Radial displacement of node i due to a unit radial load at node j
RH	Radial vector to displaced node on lug hole boundary
$RLUG$	Radius of Lug
$RPIN$	Radius of pin
d	Vertical translation of lug
t	Thickness of lug.

1. INTRODUCTION

The pin-loaded lug shown in Figure 1 is a common form of connection in aircraft structures. Until recently, the stress analysis of a lug was usually carried out in a rather simple fashion consideration usually being given only to its ultimate strength which was assessed by assuming simple stress distributions possibly modified by empirical factors. However, when considering the fatigue performance of a lug, or its strength in a cracked condition, an accurate knowledge of the stress distribution is required.

When the contact pressures applied by the pin to the lug are known then the stress analysis of the lug can be carried out using the finite element method. It has been often assumed that the contact pressure p, for a lug with the force applied along the centre line, is given by

$$p = (2P/\pi Rt)\cos\theta \qquad |\theta| \leqslant \pi/2 \qquad (1)$$

$$p = 0 \qquad |\theta| > \pi/2$$

where P is the Pin load

R is the radius of the pin

t is the thickness of the lug

θ is the angular Co-ordinate shown in Figure 2.

Intuitively, it might be expected that the actual contact pressure would resemble that given by equation (1). However equation (1) has two important defects:

1) It does not include the influence of flexibility of the pin and lug on the contact pressure.
2) The area of contact between pin and lug is assumed fixed, no allowance being made for changing areas of contact between pin and lug as a result of the type of fit or size of load applied to the pin.

Also, experimental results, reference (1), have shown that the lug stresses and strains vary non-linearly with pin load whilst equation (1) predicts a linear variation.

A method for determining the contact pressures for the case of flexible lug loaded by a rigid pin is described in references (2) and (3). A procedure in which the flexibility of both the lug and the pin is considered is given in reference (1). Both of these methods use the finite element approach. Reference (4) gives details of a photo-elastic investigation and provides some data which can be compared with theoretical results.

The present work arose out of the need to develop an accurate method for lug stress analysis which could be used in conjunction with an existing general purpose finite element program described in reference (5). The method is similar in principle to that described in references (2) and (3) but differs in the details of the computer implementation. It is also restricted to the case of a flexible lug loaded by a rigid pin. This is considered a reasonable approximation for an aluminium alloy lug loaded by a steel pin which is a common situation in aircraft structures. Also, it is assumed that frictional forces between the pin and the lug can be ignored and that the problem can be treated as a two-dimensional (plane stress) one. A particular lug is considered here for the case of neat, clearance and interference fit pins. For the neat fit pin the theoretical results are compared with some strain gauge results.

2. METHOD

2.1 Description of the lug

The method is described by its application to the particular lug shown in Figure 3; this is

of 7079–T6 aluminium alloy and formed part of a rudder actuator fitting of a large transport aircraft. Relevant properties of the alloy lug were taken to be

$$\text{Young's modulus } E = 71\cdot02 \times 10^3 \text{ MPa}$$

$$\text{Poisson's ratio } \nu = 0\cdot32$$

The line of action of the pin load is taken to lie along the centre line of the lug. The straight end of the lug is constrained in a way that leads to a uniform stress being applied at that end. Since the structure is symmetric about the centre line only half of it need be considered in the analysis. The finite element idealization of the lug based on linear strain triangles is shown in Figure 4; also shown is the cartesian co-ordinate system which has its origin set at the centre of the lug hole. On the inside of the lug hole are a series of boundary nodes at which forces and displacements between the pin and lug are to be considered. These nodes are numbered 1 to 17. The method, involves an iterative procedure, which determines the forces required at these boundary nodes to produce prescribed displacements: this is achieved by setting up a matrix of influence coefficients which defines the flexibility of the lug. In the following, as far as possible, the notation is chosen to agree with that used in the computer program.

2.2 Matrix of Influence Coefficients

The radial force applied at boundary node j is denoted by P_{Rj} ($j = 1$, $NPOINT$); this is taken to be positive when applying pressure on the lug. Also the x and y displacements at boundary node i are denoted by $DISPX_i$ and $DISPY_i$ ($i = 1$, $NPOINT$). The following matrix equations relate these quantities:

$$\{DISPX\} = [XA]\{P_R\} \tag{2}$$

$$\{DISPY\} = [YA]\{P_R\} \tag{3}$$

where $[XA]$ and $[YA]$ are square matrices of order $NPOINT \times NPOINT$. A typical element, XA_{ij}, of the first matrix is simply the value of $DISPX_i$ for $P_{Rj} = 1$ with all other values of P_R equal to zero; an analogous interpretation holds for YA_{ij}. These matrices, $[XA]$ and $[YA]$, can be determined from a finite element analysis for $NPOINT$ load cases, each case corresponding to a unit radial load at one node.

It is more convenient to define a single matrix $[A]$ relating radial displacements δ_{Ri} (taken positive when directed outwards from the origin) to the radial loads; this is given by

$$\{\delta_R\} = [A]\{P_R\} \tag{4}$$

Matrix $[A]$ can be obtained from $[XA]$ and $[YA]$. Referring to Figure 5, the radial distance to node i after its displacement due to a unit radial load at node j is given by

$$RDIS_{ij} = \sqrt{\{(XCOORD_i + XA_{ij})^2 + (YCOORD_i + YA_{ij})^2\}} \tag{5}$$

where $XCOORD_i$ and $YCOORD_i$ are X and Y co-ordinates of point i. The ijth element of $[A]$ is simply the displacement of node i for this loading:

$$A_{ij} = RDIS_{ij} - RLUG \tag{6}$$

where $RLUG$ is the radius of the hole.

It is necessary to obtain the radial loads around the lug in terms of the radial displacements. This requires inversion of matrix $[A]$ and leads to the equation

$$\{P_R\} = [A]^{-1}\{\delta_R\} \tag{7}$$

2.3 Initial Load distribution

To begin, it is necessary to assume an initial distribution of contact pressure. The distribution given by equation (1) is assumed and is referred to as the 'Sinusoidal distribution'. Replacing the distributed loads by discrete radial loads P_i at the appropriate boundary nodes the corresponding cartesian displacements $DISPX_i$ and $DISPY_i$ at all boundary nodes are found from equations (2) and (3).

2.4 Establishing compatibility in displacement of Pin and Lug

Generally, the displacements calculated above will not be compatible, either because they involve some parts of the lug lying inside the pin boundary or because they give a separation between pin and lug at points where a non-zero contact pressure has been assumed. This incompatibility is demonstrated in Figure 6, where the position of the lug hole prior to loading and its (exaggerated) shape subsequent to an applied load are both shown. Here the pin is shown as a dotted outline and corresponds to the case of an interference fit. The fit is denoted by F and is based on the difference in radii between pin and hole; it is positive for clearance. Hence the pin radius is given by

$$RPIN = RLUG - F \tag{8}$$

After loading, the elongated shape of the lug hole has undergone a maximum Y displacement $DISPY_1$ at boundary node 1 which is at the vertex of the lug. This point is now at a radial distance, d, from the corresponding point on the pin, where d is given by

$$d = F - DISPY_1 \tag{9}$$

The deflected shape of the lug is translated vertically an amount d such that there is zero relative displacement between the bottom of the pin and the bottom of the deflected lug shape. Consider the displacement of boundary node i shown in Figure 7 whose co-ordinates are $XCOORD_i$, $YCOORD_i$. Under an applied loading, node i is displaced an amount $DISPX_i$, $DISPY_i$; after a vertical translation d, the cartesian co-ordinates are given by:

$$XCOORD_i + DISPX_i \tag{10}$$

$$YCOORD_i + DISPY_i + F - DISPY_1 \tag{11}$$

Hence the radial distance from the centre of the pin to the boundary node i on the deflected lug is given by

$$RH_i = \sqrt{\{(XCOORD_i + DISPX_i)^2 + (YCOORD_i + DISPY_i + F - DISPY_1)^2\}} \tag{12}$$

Thus, to make boundary node i conform to the rigid shape of the pin a radial displacement δ_{Ri} must be applied; this is given by:

$$\delta_{Ri} = RPIN - RH_i \tag{13}$$

For the purposes of determining the required radial corrections it is necessary to establish the length over which the lug and pin are in contact. It is assumed that the pin and lug are in contact from node 1 up to a node designated ICL. For a neat fitting pin, ICL is the node which has angular co-ordinates of $\pi/2$. In the case of clearance or interference fits, ICL is the next highest node to that at which the current pressure distribution is down to zero. Corrective displacements given by equation (13) are applied to all nodes up to ICL and any higher numbered nodes for which δ_{Ri} is positive. Beyond ICL all nodes for which δ_{Ri} is negative and thus there is a separation between pin and lug, no corrective displacements are applied and δ_{Ri} is set to zero. Note however that negative values of δ_{Ri} may be applied within the contact length.

In Figure 6 the segment AB is the portion of the lug over which the corrective displacements are applied. Over segment BC there is no contact between pin and lug and hence no corrections are applied.

2.5 Modification of load Distribution

The loads that result from the corrective displacements are obtained from equation (7), and are added to the originally assumed load distribution. No corrective loads are added at points for which the corrective displacements are zero. Hence the modified load distribution $\{P_M\}$ is given by:

$$\{P_M\} = [A]^{-1}\{\delta_R\} + \{P\} \tag{14}$$

(In the program the inverse matrix has been overwritten on the original matrix.)

Generally this load distribution will give a different resultant pin force to that required. Before proceeding, the load distribution as given by equation (14) is scaled to return the correct

total pin force. For neat and clearance fit cases the $\{P_M\}$ are simply scaled linearly by the ratio of the required pin load to the pin load given by $\{P_M\}$. This will not, however, work for interference fits. The corrective load distribution $[A]^{-1}\{\delta_R\}$ for even small interference fits, can produce a large resultant load in the opposite direction to the applied sine load. If the magnitude of the sine load is not sufficiently large then the resultant pin force will be in the opposite direction to that required. To obtain solutions in the required direction it is necessary to scale up the initial sine load until the resultant pin load from equation (14) is just greater than the required pin load. How close the resultant load is to the required load depends on the smallness of increments in which the sine load is scaled up. These increments are usually set at 0·1 of the initial sine load.

This completes the first iteration.

2.6 Further Iterations

The load distribution just determined becomes the input for the second iteration. The corresponding deflections are found from equations (2) and (3). The corrective displacements required are found from equations (12) and (13). The modified load distribution is found from equation (14). After scaling, the third iteration begins. Iterations are continued until successive load distributions show negligible change.

3. PROGRAM

This program requires a data file *INPUT*. The form of *INPUT* is shown in Appendix I. In this data file it is necessary to specify the number of points around the lug, the number of iterations to be carried out, the type of fit and the required pin load as well as geometrical data. In addition, an initial approximate load distribution is required. A sinusoidal load distribution has been used for the results in this analysis; however a single concentrated load at the vertex of the lug will give the same results (but requiring more iterations) and is more convenient to set up in the data. Also required is a matrix of influence coefficients which, as already mentioned, is obtained from a standard finite element analysis of the lug.

For each iteration, the radial loads, the X and Y components of the radial load, the X and Y displacements, the contact pressure and pin loads are printed in file OUTPUT. Another output file is CHECK; this is simply an echo of the input data.

A listing of the program is given in Appendix II.

4. RESULTS

Distributions of contact pressure around the particular lug shown in Figure 3 have been obtained for neat, clearance and interference fits for various pin loads. Tables 1 to 6 contain the results for various fits for a pin load of 50,000 N. For comparison purposes these contact pressures are shown in Figure 8. In Tables 7 to 9 are the results for a clearance fit of 0·05 mm with varying pin loads from 25,000 N to 200,000 N; these distributions of contact pressure are plotted in Figure 9. Results for an interference fit of $-0{\cdot}04$ mm for pin loads varying from 30,000 N to 200,000 N are shown in Tables 10–12 and are plotted in Figure 10.

Returning to the standard finite element analysis, the stresses around the lug are obtained for the cases corresponding to pin loads of 50,000 N. These results are contained in Tables 13 to 18 and are plotted in Figures 11 to 16. Here, the stresses are in the polar co-ordinate system where σ_R, σ_T and σ_{RT} denote respectively the radial and tangential direct stresses and the shear stress.

Experimental data in the form of strain gauge readings are available for this lug and are shown in Table 19; these are for the case of a neat fitting pin with a pin load of 50,000 N. The location of the gauges is shown in Figure 17. These strain gauges have been placed to measure radial strains ϵ_R and tangential strains ϵ_T and correspond to radial lines through boundary nodes 1, 5 and 9 (angles of $\theta = 0^\circ$, 45° and 90° respectively). Theoretical stresses can be converted to strains by the relations:

$$\epsilon_R = (\sigma_R - \nu.\sigma_T)/E$$

$$\epsilon_T = (\sigma_T - \nu.\sigma_R)/E$$

where E is Young's modulus and ν is Poisson's ratio. These strains have been calculated and are shown in Table 20. In Figure 18 are shown the plots for these theoretical strains, the experimental strains have been superimposed on these plots and show reasonably good agreement.

In reference (4) stress concentration factors obtained from photo-elastic methods are given for various lug geometries. These stress concentration factors are for the tangential stress at the edge of the lug hole for an angle of $\theta = 90°$. In Appendix III, theoretical stress concentration factors have been calculated for clearance, neat and interference fits, the pin load being 50,000 N. For the geometry of the lug in Figure (3), the only direct comparison of results that can be made is that of a neat fit. Here the experimental value is approximately 2·4 and the trend is for higher stress concentration factors for clearance fits and lower factors for interference fits.

DISCUSSION

The procedure by which the contact load distribution is obtained in the program is an iterative one. This is due to the non-linear nature of the contact problem. Solutions tend to oscillate about the exact solution and slowly converge to it. It was found necessary to perform up to 1000 iterations until two consecutive iterations agreed closely. There were some cases for which the solution would not converge and these will be mentioned later.

To examine the influence of the type of fit on the load distribution the various load distributions corresponding to clearance, neat and interference have been plotted on Figure 8. Firstly, considering the curve for the clearance fit, it is seen that this curve exhibits a characteristic peak at $\theta = 0°$ which then drops off at 15°. This is followed by a steep increase of contact pressure to a maximum at 60°; this then reduces rapidly and the pin is free from the lug beyond 85°. In the case of a neat fit, the peaks in the curve have flattened out and the contact arc has increased. This trend continues for the cases of interference fits. With the higher interference fits the maximum contact pressure between the pin and lug increases as does the length of arc in contact. For an interference fit of −0·07 mm the contact arc is 160°.

Consider now the effect of the magnitude of the pin load on the load distribution. As the pin load is increased the area of pin and lug in contact will change, the lug tends to wrap itself around the pin to a greater extent. This is demonstrated in Figure 9. However, in the case of an interference fit, (−0·04 mm) as shown in Figure 10, the contact length decreases with increase in load.

For the case of a neat fit, use of the load distribution in our finite element model has given results that compare reasonably with experimental values. Tangential strains are within 7% of the experimental values; however there are larger discrepancies in the radial strains. Stress concentration factors obtained from photo-elasticity, reference (4), are in general agreement for cases of clearance, neat and interference fits. Specific values of stress concentration factors for clearance and interference fits for the geometry of the present lug are not given; however the trend is toward higher stress concentrations with increase of clearance and lower stress concentrations for interference fits. For the case of a neat fit the experimental value of stress concentration is within 10% of the theoretical value.

The effect of various fits on the stress distribution is now considered for a constant pin load of 50,000 N. Consider firstly the stress distribution shown in Figure 11 for the case of a neat fit. The maximum stresses are the tangential stresses on the inside of the lug hole at boundary node 9 ($\theta = 90°$). Comparison with Figure 12 for the case of a clearance fit shows that the tangential stresses at 90° are greater for the clearance than for the neat fit while the tangential stresses at 0° and 45° (are smaller for the clearance than for the neat fit). Radial stresses at $\theta = 45°$ and $\theta = 0°$ are similar for the clearance and neat fit cases, though not, of course, at $\theta = 90°$.

Comparing now the stresses for the neat fit (Fig. 11) with the stresses resulting from an interference of −0·04 mm (Fig. 13), it is apparent that the tangential stresses at $\theta = 90°$ with the interference fit are lower than those with the neat fit, while the tangential stresses at 0° and 45° are slightly greater with the interference fit as were the radial stresses. Over all, the effect of −0·04 mm interference is to reduce the maximum stresses. However for higher interference fits, as shown in Figures 14 to 16, progressively all stresses are increased including the tangential stresses at 90°.

From the point of view of minimising the stresses in the lug for a given pin load it seems

that the smaller interference fits are optimum. A plot of maximum tangential stress versus interference is shown on Figure 19. However, in the case of fatigue it is the increment of stress during a stress cycle that is important. The increment in tangential stress $\Delta\sigma_T$ has been calculated in Appendix IV and also plotted in Figure 19, this corresponds to a stress cycle starting from zero pin load. As can be seen from Figure 19 the minimum value of this increment corresponds to higher interference fits of $-0 \cdot 07$ mm; for fatigue it seems that the higher interference fits are optimum.

Factors determining the accuracy of the theoretical load distribution are now considered. In part, the accuracy is dependent on the number of points used in determining the load distribution. For clearance fits the small contact arc may result in only 7 or 8 points determining the shape of the load distribution. Also the arc length between adjacent points is relatively large in comparison with the contact arc. This makes convergence of the solution more difficult since jumps in contact length from one point to the next have a substantial effect on the shape of the load distribution. For neat and interference fits the longer contact arc ensures that more points are used to determine the solution and this improves the accuracy.

The accuracy of the load distribution is also determined by the accuracy of the individual terms A_{ij} comprising the matrix of influence coefficients and subsequent inversion. In this analysis the values of these terms were only taken to four significant figures. This was just acceptable; however six significant figures is suggested. Fortunately, no difficulty was encountered in achieving an accurate inversion of the matrix of influence coefficients. In this analysis solutions would not converge for levels of interference above $-0 \cdot 07$ mm for loads of 50,000 N or for loads lower than 30,000 N with small amounts of interference.

Loss of accuracy may also occur in the program in equations (6) and (13) where the result is the difference between two almost equal numbers. In this program satisfactory results were obtained using single precision arithmetic. The program was run a PDP-10 computer where the word length is 36 Bits and gives at least eight significant figures for single precision. For computers with wordlengths less than this, double precision is advisable.

6. CONCLUSION

A method has been developed for the solution of the non-linear pin-lug contact problem. This has allowed a finite element analysis of a pin loaded lug which has provided the stress distribution around the lug. The method is, however, restricted to the concept of a flexible lug loaded by a rigid pin. The example used of an aluminium alloy lug loaded by a steel pin appears to fit within this concept, as a comparison between experimental and theoretical result shows agrement within 7–10%.

REFERENCES

1.	White, D. J. and Enderby, L. R.	Finite-Element Stress Analysis of a non-linear problem: A connecting-rod eye loaded by means of a pin. Journal of strain analysis. Vol. 5, No. 1, 1970, pp. 177–192.
2.	Harris, H. G., Ojalvo, I. V. and Hooson, R. E.	Stress and deflection analysis of mechanically fastened joints. U.S. Air Force Flight Dynamics Laboratory. AFFDL–TR–70–49, 1970.
3.	Harris, H. G. and Ojalvo, I. O.	Simplified three dimensional analysis of mechanically fastened joints. Proceedings of the Army Symposium on Solid Mechanics, 1974. The Role of Mechanics in Design—Structural Joints. U.S. Army Materials and Research Centre AMMRC MS 74–8, 1974.
4.	Frocht, M. M. and Hill, H. N.	Stress concentration factors around a central circular hole in a plate loaded through a pin in the hole. Photoelasticity: The selected scientific papers of M. M. Frocht, edited by M. M. Leven. Pergamon Press, 1969. pp. 159–171.
5.	Callinan, R. J.	User's Manual for Dismal—A general purposes structural analysis program. Aeronautical Research Laboratories S. & M. Tech. Memo 227, Jan. 1975.
6.	—	Engineering Sciences Data Items No. 71011, Engineering Sciences Data Unit, London, May, 1971.

APPENDIX I

The data file *INPUT* requires the following:

Variables	*Format*
NPOINT, NLL, NITER	3I5
RPIN, F, ANGLE, QS, THICK	5F12·5
PLL(1)	E12·5
PS(*I*)	E12·5
XA (*I, J*)	6E12·5
YA (*I, J*)	6E12·5

where

NPOINT	is the number of points around half the lug
NLL	Set to 1; this was left in to allow several load cases to be considered at once; however the extra programming has not yet been implemented.
NITER	is the number of iterations to be made
RPIN	is the radius of the pin
F	is the fit of the pin in the lug, negative for interference
ANGLE	is the angle in degrees between adjacent points
QS	is the total pin load corresponding to the sine load distribution.
THICK	is the thickness of the lug
PLL(1)	Set this to the required pin load for the complete lug.
PS(*I*)	Radial force at point *I* due to sinusoidal loading
XA (*I, J*)	*X* displacement at point *I* due to a unit radial load at point *J*.
YA (*I, J*)	*Y* displacement at point *I* due to a unit radial load at point *J*.

APPENDIX II BEST AVAILABLE COPY

```
C       PROGRAM TO SOLVE CONTACT PROBLEM BETWEEN PIN AND LUG
C
C
        COMMON/BLOCK1/NPOINT,NLL,NITER,KKK,PLL(10),SCALE
        COMMON/PRINTR/JSCA,JSCB,JSCC
        INTEGER TAPNM1(2),TAPNM2(2),TAPNM3(2)
        DATA TAPNM1/6HINPUT$/,TAPNM2/6HCHECK$/,TAPNM3/7HOUTPUT$/
        DATA JSCA/1/,JSCB/2/,JSCC/3/
        OPEN(UNIT=JSCA,FILE=TAPNM1,ACCESS='SEQIN')
        OPEN(UNIT=JSCB,FILE=TAPNM2,ACCESS='SEQOUT')
        OPEN(UNIT=JSCC,FILE=TAPNM3,ACCESS='SEQOUT')
        OPEN(UNIT=4,FILE='DISDAT$')
        SCALE=.10
C
        CALL READ
C
        CALL SINE(NPOINT)
C
        CALL COORD
C
        CALL MATA
C
C
        DO 1000 KKK=1,NITER

C
500     CALL PDINC
C
        CALL RAD
C
        CALL RLOAD
C
        CALL TLOAD(I)
        IF(I.EQ.1)GOTO 500
C
        CALL DISP
C
        CALL WRITE
C
1000    CONTINUE
        END
        SUBROUTINE READ
        COMMON/BLOCK1/NPOINT,NLL,NITER,KKK,PLL(10),SCALE
        COMMON/BLOCK2/XA(20,20),YA(20,20),A(20,20)
        COMMON/BLOCK4/XDISPS(20),YDISPS(20),PS(20)
        COMMON/BLOCK6/RPIN,F,ANGLE,QS,QT,R(20),THICK
        COMMON/PRINTR/JSCA,JSCB,JSCC
10      FORMAT(3I5)
20      FORMAT(7F12.5)
30      FORMAT(6E12.5)
C
C       READ IN NUMBER OF POINTS, PIN LOAD AND NUMBER OF ITERATIONS
C
        READ(JSCA,10)NPOINT,NLL,NITER
        WRITE(JSCB,10)NPOINT,NLL,NITER
C
C       READ IN RADIUS OF PIN, FIT ,PIN LOAD, QS AND THICKNESS OF LUG
C       FIT IS NEGATIVE FOR INTERFERENCE.
C
        READ(JSCA,20)RPIN,F,ANGLE,QS,THICK
```

```
      WRITE(JSCB,20)RPIN,F,ANGLE,QS,THICK
C
C     READ IN PARTICULAR    PIN    LOADS
C
      READ(JSCA,30)(PLL(I),I=1,NLL)
      WRITE(JSCB,30)(PLL(I),I=1,NLL)
      DO 100 I=1,NPOINT
C
C     READ IN RADIAL LOADS FOR SINUSOIDAL LOADING QS
C     ( OR ANY OTHER APPROXIMATE LOADING I.E. CONCENTRATED
C     LOAD AT VERTEX OF LUG WILL WORK )
C
      READ(JSCA,30)PS(I)
100   WRITE(JSCB,30)PS(I)
C
C     READ IN X AND Y DISPLACEMENTS OF EACH POINT DUE TO UNIT LOADS
C
      DO 200 I=1,NPOINT
      READ(JSCA,30)(XA(I,J),J=1,NPOINT)
      WRITE(JSCB,30)(XA(I,J),J=1,NPOINT)
      READ(JSCA,30)(YA(I,J),J=1,NPOINT)
200   WRITE(JSCB,30)(YA(I,J),J=1,NPOINT)
      RETURN
      END
      SUBROUTINE SINE(NPOINT)
      COMMON/BLOCK2/XA(20,20),YA(20,20),A(20,20)
      COMMON/BLOCK4/XDISPS(20),YDISPS(20),PS(20)
C
C     FORM DISPLACEMENTS CORRESPONDING TO RADIAL SINE LOAD
C     OR ANY OTHER APPROXIMATE LOAD DISTRIBUTION
C
      DO 200 I=1,NPOINT
      SUMX=0.
      SUMY=0.
      DO 100 J=1,NPOINT
      SUMX=SUMX+XA(I,J)*PS(J)
100   SUMY=SUMY+YA(I,J)*PS(J)
      XDISPS(I)=SUMX
      YDISPS(I)=SUMY
200   CONTINUE
      RETURN
      END
      SUBROUTINE COORD
      COMMON/BLOCK1/NPOINT,NLL,NITER,KKK,PLL(10),SCALE
      COMMON/BLOCK3/XCOORD(20),YCOORD(20)
      COMMON/BLOCK6/RPIN,F,ANGLE,QS,QT,R(20),THICK
C
C     RLUG IS RADIUS OF HOLE
C
      RLUG=RPIN+F
      THETA=0.
C
C     NOW CALCULATE COORDS OF UNDEFLECTED LUG
C
      DO 100 I=1,NPOINT
      XCOORD(I)= RLUG*SIND(THETA)
      YCOORD(I)=-RLUG*COSD(THETA)
100   THETA=THETA+ANGLE
      RETURN
      END
```

```
      SUBROUTINE MATA
      COMMON/BLOCK1/NPOINT,NLL,NITER,KKK,PLL(10),SCALE
      COMMON/BLOCK2/XA(20,20),YA(20,20),A(20,20)
      COMMON/BLOCK3/XCOORD(20),YCOORD(20)
C
C     MATRIX A IS A SET OF RADIAL DISPLACEMENTS FOR UNIT
C     RADIAL LOADS.
C
      DO 200 I=1,NPOINT
      DO 200 J=1,NPOINT
C
C     WE MUST NOW DETERMINE WHICH RADIAL DISPLACEMENTS
C     ARE POSITIVE AND NEGATIVE
C     RADIAL COMPRESSION IS TAKEN TO BE POSITIVE.
C     R IS RADIAL VECTOR TO POINT
C     RDIS IS RADIAL VECTOR TO DISPLACED POINT
C
      R=SQRT((XCOORD(I))**2+(YCOORD(I))**2)
      RDIS=SQRT((XCOORD(I)+XA(I,J))**2+(YCOORD(I)+YA(I,J))**2)
      A(I,J)=RDIS-R
200   CONTINUE
      CALL GENINV(A,NPOINT,20,D,IRROR,CONO)
      RETURN
      END
      SUBROUTINE GENINV(A,N,M,D,IRROR,CONO)
C
C     THIS INVERSION ROUTINE WAS WRITTEN BY D.W.G. MOORE
C     COMPUTING CENTRE, UNIVERSITY OF WESTERN AUSTRALIA
C
      DIMENSION A(M,M),IPIV(100),IND(100,2)
      IF(N.LE.0.OR.N.GT.M.OR.M.GT.100) GOTO 80
      CALL OVERFL(JJJ)
      ASSIGN 7777 TO GOBACK
      GOTO 7779
7777  D=1.0
      IRROR=0
      DO 10 I=1,N
10    IPIV(I)=0
      DO 220 I=1,N
      AMAX=0.0
C
C     SEARCH SUB-MATRIX FOR LARGEST ELEMENT AS PIVOT
C
      DO 70 J=1,N
      IF(IPIV(J))102,30,70
30    DO 60 K=1,N
      IF(IPIV(K)-1)40,60,103
C
C     THIS ROW HAS BEEN A PIVOT
C
40    IF(ABS(A(J,K)).LE.AMAX)GOTO 60
50    IROW=J
      ICOL=K
      AMAX=ABS(A(J,K))
60    CONTINUE
70    CONTINUE
C
C     PIVOT FOUND
C
      IPIV(ICOL)=IPIV(ICOL)+1
```

```
90      IF(IROW.EQ.ICOL)GOTO 130
C
C       MAKE PIVOT A DIAGONAL ELEMENT BY ROW INTERCHANGE
C
95      D=-D
        DO 100 K=1,N
        AMAX=A(IROW,K)
        A(IROW,K)=A(ICOL,K)
100     A(ICOL,K)=AMAX
130     IND(I,1)=IROW
        IND(I,2)=ICOL
        AMAX=A(ICOL,ICOL)
        IF(D.LT.0.1E-15)D=0.
        IF(AMAX.LT.0.1E-15)AMAX=0.
        D=D*AMAX
        A(ICOL,ICOL)=1.0
C
C       DIVIDE ROW BY PIVOT
C
        DO 140 K=1,N
140     A(ICOL,K)=A(ICOL,K)/AMAX
        DO 220 J=1,N
        IF(J.EQ.ICOL)GOTO 220
180     AMAX=A(J,ICOL)
        A(J,ICOL)=0.
        DO 190 K=1,N
190     A(J,K)=A(J,K)-A(ICOL,K)*AMAX
220     CONTINUE
C
C       FOR INVERSE OF A, INTERCHANGE COLUMNS
C
230     DO 260 I=1,N
        J=N+1-I
240     IROW=IND(J,1)
        IF(IND(J,1).EQ.IND(J,2))GOTO 260
        ICOL=IND(J,2)
        DO 250 K=1,N
        AMAX=A(K,IROW)
        A(K,IROW)=A(K,ICOL)
250     A(K,ICOL)=AMAX
260     CONTINUE
270     CALL OVERFL(JJJ)
        IF(JJJ.NE.2)IRROR=1
        ASSIGN 8000 TO GOBACK
        CONSAV=CONO
        GOTO 7779
8000    CONO=CONSAV*CONO
        RETURN
80      IRROR=2
        RETURN
102     IRROR=3
        RETURN
103     CONTINUE
        IRROR=4
        RETURN
7779    CONO=0.
        DO 7780 I=1,N
        DO 7780 J=1,N
7780    CONO=CONO+A(I,J)**2
        CONO=SQRT(CONO)
```

```
      GOTO GOBACK
      END
      SUBROUTINE PDINC
      COMMON/BLOCK1/NPOINT,NLL,NITER,KKK,PLL(10),SCALE
      COMMON/BLOCK4/XDISPS(20),YDISPS(20),PS(20)
      COMMON/BLOCK5/DISPX(20),DISPY(20),P(20)
C
C     THIS ROUTINE UPDATES LOADS AND DISPLACEMENTS
C
      IF(KKK.GT.1)GOTO 200
      DO 100 I=1,NPOINT
      DISPX(I)=SCALE*XDISPS(I)
      DISPY(I)=SCALE*YDISPS(I)
100   P(I)=SCALE*PS(I)
200   RETURN
      END
      SUBROUTINE RAD
      COMMON/BLOCK1/NPOINT,NLL,NITER,KKK,PLL(10),SCALE
      COMMON/BLOCK3/XCOORD(20),YCOORD(20)
      COMMON/BLOCK5/DISPX(20),DISPY(20),P(20)
      COMMON/BLOCK6/RPIN,F,ANGLE,QS,QT,R(20),THICK
      IF(F.GT.0.)GOTO 140
      IF(F.LT.0.)GOTO 350
C
C     NEAT FIT - CONTACT LENGTH OVER 90 DEGREES
C
      ICL=10
      GOTO 550
C
C     FIND CONTACT LENGTH FOR CLEARANCE
C
140   I=0
150   I=I+1
      IF(P(I).EQ.0.)GOTO 250
      IF(I.EQ.NPOINT)GOTO 200
      GOTO 150
200   ICL=NPOINT
      GOTO 300
250   ICL=I+1
C
C     SHOULD BE ICL=I , HOWEVER ICL=I+1 ALLOWS SOLUTION TO CONVERGE
C     NO ERROR IN THIS ASSUMPTION PROVIDED SOLUTION DOES CONVERGE
C
300   CONTINUE
      GOTO 550
C
C     FIND CONTACT LENGTH FOR INTERFERENCE
C
350   I=0
400   I=I+1
      IF(P(I).EQ.0.)GOTO 500
      IF(I.EQ.NPOINT)GOTO 450
      GOTO 400
450   ICL=NPOINT
      GOTO 550
500   ICL=I+1
550   CONTINUE
C
C     FORM RADIAL DISPLACEMENTS THAT ARE TO BE APPLIED TO LUG
C
```

```
      THETA=Ø.
      DRPIN=RPIN
      DO 1ØØ I=1,NPOINT
      THETA=THETA+11.25
      RH=SQRT((XCOORD(I)+DISPX(I))**2+(YCOORD(I)+DISPY(I)
     1 -DISPY(1)+F)**2)
      R(I)=RPIN-RH
C
C     REMOVE TENSILE RADIAL DISPLACEMENT CORRECTIONS
C     OUTSIDE CONTACT LENGTH
C
      IF(I.LT.ICL)GOTO 1ØØ
      IF(RPIN.LT.RH)R(I)=Ø.
1ØØ   CONTINUE
      RETURN
      END
      SUBROUTINE RLOAD
      COMMON/BLOCK1/NPOINT,NLL,NITER,KKK,PLL(1Ø),SCALE
      COMMON/BLOCK2/XA(2Ø,2Ø),YA(2Ø,2Ø),A(2Ø,2Ø)
      COMMON/BLOCK5/DISPX(2Ø),DISPY(2Ø),P(2Ø)
      COMMON/BLOCK6/RPIN,F,ANGLE,QS,QT,R(2Ø),THICK
C
C     NOW FORM RADIAL LOADS
C
      ISW=Ø
      DO 2ØØ I=1,NPOINT
      SUM=Ø.
      DO 1ØØ J=1,NPOINT
1ØØ   SUM=SUM+A(I,J)*R(J)
C
C     REMOVE LOADS FOR WHICH
C     RADIAL DISPLACEMENTS ARE ZERO
C
      IF(R(I).EQ.Ø.)SUM=Ø.
C
C     ADD INITIAL LOAD TO OBTAIN TOTAL LOAD
C
      P(I)=P(I)+SUM
C
C     REMOVE TENSILE LOADS
C
      IF(P(I).LT.Ø.)P(I)=Ø.
      IF(P(I).EQ.Ø.)ISW=1
      IF(ISW.EQ.1)P(I)=Ø.
2ØØ   CONTINUE
      RETURN
      END
      SUBROUTINE TLOAD(K)
      COMMON/BLOCK1/NPOINT,NLL,NITER,KKK,PLL(1Ø),SCALE
      COMMON/BLOCK5/DISPX(2Ø),DISPY(2Ø),P(2Ø)
      COMMON/BLOCK6/RPIN,F,ANGLE,QS,QT,R(2Ø),THICK
C
C     THIS ROUTINE ADJUSTS THE  LOAD
C     DISTRIBUTION TO GIVE THE REQUIRED TOTAL LOAD
C
      K=Ø
      ICOUNT=Ø
5Ø    ICOUNT=ICOUNT+1
      THETA=Ø.
      QT=P(1)
```

```
          DO 100 I=2,NPOINT
          THETA = THETA+ANGLE
          QT=QT+P(I)*(COSD(THETA))
100       CONTINUE
          IF(KKK,GT.1)GOTO 250
C
C         THE THEORY HERE IS THAT WE ARE CLOSE ENOUGHT TO THE LOAD
C         TO MAKE AN ASSUMPTION OF LINEAR LOAD WITH LOAD DISTRIBUTION
C         RELATIONSHIP
C
          IF(F,LT.0.)GOTO 350
C
C         USE A FACTOR X FOR NEAT OR CLEARANCE FITS
C
250       X=ABS(PLL(1)/(QT*2.))
          DO 200 I=1,NPOINT
200       P(I)=P(I)*X
          IF(ICOUNT.GT,100)GOTO 300
          IF(X,LT.0.99,OR.X.GT,1.01)GOTO 50
300       RETURN
C
C         USE FACTOR SCALE FOR INTERFERENCE FITS
C
350       CONTINUE
          QTT=2.*QT
          IF(QTT,LT.PLL(1))GOTO 400
C
C         TAKE FIRST VALUE GREATER THAN PLL(1)
C
          GOTO 300
C
C         SCALE IS NOW SET FOR ALL OTHER ITERATIONS
C
400       IF(KKK,GT.1)GOTO 300
          SCALE=SCALE+,1
          IF(SCALE.GT.100.)GOTO 300
          K=1
          RETURN
          END
          SUBROUTINE DISP
          COMMON/BLOCK1/NPOINT,NLL,NITER,KKK,PLL(10),SCALE
          COMMON/BLOCK2/XA(20,20),YA(20,20),A(20,20)
          COMMON/BLOCK5/DISPX(20),DISPY(20),P(20)
C
C         FORM SET OF DISPLACEMENTS CORRESPONDING TO LOAD DISTRIBUTION
C
          DO 200 I=1,NPOINT
          SUMX=0.
          SUMY=0.
          DO 100 J=1,NPOINT
          SUMX=SUMX+XA(I,J)*P(J)
100       SUMY=SUMY+YA(I,J)*P(J)
          DISPX(I)=SUMX
200       DISPY(I)=SUMY
          RETURN
          END
          SUBROUTINE WRITE
          COMMON/BLOCK1/NPOINT,NLL,NITER,KKK,PLL(10),SCALE
          COMMON/BLOCK5/DISPX(20),DISPY(20),P(20)
          COMMON/BLOCK6/RPIN,F,ANGLE,QS,QT,R(20),THICK
```

```
      COMMON/PRINTR/JSCA,JSCB,JSCC
      DIMENSION AP(20),APX(20),APY(20),APRESS(20),FX(40),FY(40)
      KMI=1000
      IF(KKK.LT.KMI)GOTO 200
10    FORMAT(' ITERATION ',I4,12X,'FORCE  N,',12X,
     1 'DISPLACEMENT  MM,',12X,'CONTACT PRESSURE  MPA,'//)
20    FORMAT('   PIN LOAD ',2X,F10.2,20X,' FIT ',2X,F10.6,20X,
     1 ' RPIN ',2X,F10.6//)
40    FORMAT(' POINT',5X,'RLOAD',9X,'XLOAD ',8X,' YLOAD ',8X,
     1 ' XDISPL',8X,' YDISPL',4X,'CONTACT PRESSURE'//)
50    FORMAT(2X,I4,F13.2,2(2X,F13.2),2(2X,E13.6),2X,F13.2)
60    FORMAT(1H ///)
C
C     F1 AND F2 ARE CONVERSION FACTORS FOR UNITS
C
      F1=4.44822
      F2=25.4
      AP(1)=F1*(2.0*P(1))
      DO 90 I=2,NPOINT
90    AP(I)=F1*(P(I))
      QTT=F1*(2.0*QT)
      T=F2*(THICK)
      RL=F2*(RPIN+F)
C
C     NOW FORM CONTACT PRESSURE
C
      S=57.296/(RL*ANGLE*T)
      DO 95 I=1,NPOINT
95    APRESS(I)=AP(I)*S
      WRITE(JSCC,10)KKK
      FIT=F2*(F)
      RP=F2*(RPIN)
      WRITE(JSCC,20)QTT,FIT,RP
      WRITE(JSCC,40)
      THETA=0.
      DO 100 I=1,NPOINT
      APX(I)= AP(I)*SIND(THETA)
      APY(I)=-AP(I)*COSD(THETA)
      THETA=THETA+ANGLE
      DX=F2*(DISPX(I))
      DY=F2*(DISPY(I))
100   WRITE(JSCC,50)I,AP(I),APX(I),APY(I),DX,DY,APRESS(I)
      WRITE(JSCC,60)
200   RETURN
      END
```

APPENDIX III

Stress concentration factors

Referring to Figure 4 with σ_T^9 being the tangential stress at point 9, then the stress concentration factor is given by:

$$K = \frac{\sigma_T^9}{\frac{P}{A}}$$

where P/A is the nominal stress

Referring to the dimensions given in Figure 3, the minimum cross sectional area of the lug is given by:

$$A = 2 \times (29\cdot591 - 16\cdot866) \times 12\cdot700 \times 10^{-6}\,\mathrm{m}^2$$

$$= 3\cdot232 \times 10^{-4}\,\mathrm{m}^2$$

For a pin load of 50,000 N, the nominal stress is $P/A = 1\cdot547 \times 10^8$ Pa.

For the pin load of 50,000 N the following stress concentration factors are given for various fits.

Fit (mm)	σ_T^9 (MPa)	K
0·05	395·9	2·559
0·00(Neat)	333·4	2·155
−0·04	230·8	1·492
−0·05	236·7	1·530
−0·06	252·6	1·632
−0·07	279·4	1·806

The experimental value of K for a neat fit given in reference (4) is approximately 2·4.

APPENDIX IV

Tangential Stresses due to Interference only, zero pin load

From reference (6) the tangential stress at the pin-lug interface due to an interference pin with zero pin load is given by:

$$\frac{\sigma_T}{Ee} = \frac{q}{Ee}\left[1 + \left(\frac{d}{w}\right)^2\right]$$

and

$$\frac{q}{Ee} = \frac{1}{2 + \left[\dfrac{E(1-\nu_1)}{E_1} - (1-\nu)\right]\left[1 - \left(\dfrac{d}{w}\right)^2\right]}$$

where E_1, ν_1 are Youngs modulus and Poisson's ratio for pin

E, ν are Youngs modulus and Poisson's ratio for lug

d is diameter of lug hole

w is width of lug

e $= 2F/d$.

Here we take $E_1 = 206 \cdot 8 \times 10^3$ MPa and $\nu_1 = 0 \cdot 30$, while E and ν have the same values as previously given.

Substituting

$$\sigma_T = 32 \cdot 75 \times 10^2 \times F \quad \text{MPa}$$

Interference (mm)	σ_T (MPa)
−0·04	131·0
−0·05	163·7
−0·06	196·7
−0·07	229·3

The following maximum values of σ_T have been extracted from tables 13–20; from these values $\Delta\sigma_T$ is calculated. $\Delta\sigma_T$ is given by:

$$\Delta\sigma_T = \sigma_{T\max} - \sigma_T \text{ (zero pin load)}$$

Fit (mm)	$\sigma_{T\max}$(MPa)	$\Delta\sigma_T$ (MPa)
0·05	395·9	395·9
0·00	333·4	333·4
−0·04	230·8	99·8
−0·05	236·7	73·0
−0·06	263·3	66·8
−0·07	294·9	65·6

TABLE 1

Results for Lug with Neat Fit Pin; Pin Load of 50,000 N

Iteration 1000 Pin Load 49997·04	Force N		Displacement mm Fit 0·000000			Contact pressure MPa RPIN 16·865600
POINT	RLOAD	XLOAD	YLOAD	XDISPL	YDISPL	Contact Pressure
1	4505·87	0·00	−4505·87	0·000000E + 00	−0·196690E + 00	107·14
2	4642·66	905·74	−4553·45	0·951496E − 02	−0·194793E + 00	110·39
3	4670·51	1787·33	−4314·99	0·172245E − 01	−0·189541E + 00	111·05
4	4910·07	2727·89	−4082·57	0·232596E − 01	−0·181114E + 00	116·75
5	5157·16	3646·66	−3646·66	0·265509E − 01	−0·170068E + 00	122·62
6	5524·04	4593·07	−3068·99	0·266389E − 01	−0·156678E + 00	131·35
7	5553·97	5131·20	−2125·41	0·226021E − 01	−0·141812E + 00	132·06
8	4895·64	4801·58	−955·09	0·139372E − 01	−0·125744E + 00	116·41
9	1798·66	1798·66	0·00	−0·243428E − 03	−0·109270E + 00	42·77
10	0·00	0·00	0·00	−0·102270E − 01	−0·938571E − 01	0·00
11	0·00	0·00	0·00	−0·134653E − 01	−0·795370E − 01	0·00
12	0·00	0·00	0·00	−0·136492E − 01	−0·671178E − 01	0·00
13	0·00	0·00	0·00	−0·119950E − 01	−0·566495E − 01	0·00
14	0·00	0·00	0·00	−0·941759E − 02	−0·485897E − 01	0·00
15	0·00	0·00	0·00	−0·642384E − 02	−0·427444E − 01	0·00
16	0·00	0·00	0·00	−0·326893E − 02	−0·392940E − 01	0·00
17	0·00	0·00	0·00	0·000000E + 00	−0·381245E − 01	0·00

TABLE 2

Results for Lug with 0.05 mm Clearance Fit Pin; Pin Load of 50,000 N

Iteration 1000 Pin Load 50000·29	Force N		Displacement mm Fit 0·050000			Contact Pressure MPa RPIN 16·865600
POINT	RLOAD	XLOAD	YLOAD	XDISPL	YDISPL	Contact Pressure
1	5524·13	0·00	−5524·13	0·000000E + 00	−0·215470E + 00	130·96
2	4142·67	808·20	−4063·07	0·702052E − 02	−0·210352E + 00	98·21
3	4483·26	1715·67	−4141·99	0·129250E − 01	−0·204380E + 00	106·29
4	4792·16	2662·38	−3984·54	0·167979E − 01	−0·194739E + 00	113·61
5	5446·08	3850·96	−3850·96	0·179861E − 01	−0·182691E + 00	129·11
6	6181·08	5139·38	−3434·02	0·153651E − 01	−0·167858E + 00	146·54
7	5696·18	5262·58	−2179·83	0·681776E − 02	−0·150476E + 00	135·04
8	2991·55	2934·07	−583·62	−0·795791E − 02	−0·130920E + 00	70·92
9	0·00	0·00	0·00	−0·219930E − 01	−0·111815E + 00	0·00
10	0·00	0·00	0·00	−0·264463E − 01	−0·941771E − 01	0·00
11	0·00	0·00	0·00	−0·263577E − 01	−0·787759E − 01	0·00
12	0·00	0·00	0·00	−0·234662E − 01	−0·656684E − 01	0·00
13	0·00	0·00	0·00	−0·191225E − 01	−0·547804E − 01	0·00
14	0·00	0·00	0·00	−0·143225E − 01	−0·465039E − 01	0·00
15	0·00	0·00	0·00	−0·947811E − 02	−0·405508E − 01	0·00
16	0·00	0·00	0·00	−0·474919E − 02	−0·370524E − 01	0·00
17	0·00	0·00	0·00	0·000000E + 00	−0·358739E − 01	0·00

TABLE 3

Results for Lug with −0.04 mm Interference Fit Pin; Pin Load of 50,000 N

Iteration 1000 Pin Load		Force N 50000·14	Displacement mm Fit −0·040000			Contact Pressure MPa RPIN 16·865600
POINT	RLOAD	XLOAD	YLOAD	XDISPL	YDISPL	Contact Pressure
1	5583·63	0·00	−5583·63	0·000000E + 00	−0·177726E + 00	133·08
2	5156·83	1006·05	−5057·74	0·127237E − 01	−0·174835E + 00	122·91
3	5141·91	1967·72	−4750·50	0·239380E − 01	−0·169763E + 00	122·55
4	5187·61	2882·08	−4313·34	0·338744E − 01	−0·161714E + 00	123·64
5	5221·98	3692·50	−3692·50	0·416727E − 01	−0·151439E + 00	124·46
6	5269·62	4381·53	−2927·65	0·469185E − 01	−0·139153E + 00	125·60
7	5181·78	4787·34	−1982·98	0·490185E − 01	−0·125946E + 00	123·50
8	5143·48	5044·65	−1003·44	0·478904E − 01	−0·112266E + 00	122·59
9	4832·84	4832·84	0·00	0·431661E − 01	−0·988610E − 01	115·19
10	3931·72	3856·17	767·04	0·348518E − 01	−0·868428E − 01	93·71
11	1967·21	1817·47	752·82	0·235865E − 01	−0·772365E − 01	46·89
12	0·00	0·00	0·00	0·130728E − 01	−0·692049E − 01	0·00
13	0·00	0·00	0·00	0·752924E − 02	−0·604761E − 01	0·00
14	0·00	0·00	0·00	0·415131E − 02	−0·533776E − 01	0·00
15	0·00	0·00	0·00	0·209156E − 02	−0·480553E − 01	0·00
16	0·00	0·00	0·00	0·876236E − 03	−0·448569E − 01	0·00
17	0·00	0·00	0·00	0·000000E + 00	−0·437522E − 01	0·00

TABLE 4

Results for Lug with −0.05 mm Interference Fit Pin; Pin Load of 50,000 N

Iteration 1000 Pin Load	Force N 49989·05		Displacement mm Fit −0·050000			Contact Pressure MPa RPIN 16·865600
POINT	RLOAD	XLOAD	YLOAD	XDISPL	YDISPL	Contact Pressure
1	5806·61	0·00	−5806·61	0·000000E + 00	−0·178028E + 00	138·48
2	5506·34	1074·23	−5400·54	0·138761E − 01	−0·175321E + 00	131·32
3	5445·08	2083·74	−5030·59	0·261149E − 01	−0·170098E + 00	129·86
4	5475·96	3042·28	−4553·09	0·371246E − 01	−0·161847E + 00	130·59
5	5539·11	3916·74	−3916·74	0·460359E − 01	−0·151354E + 00	132·10
6	5526·30	4594·95	−3070·25	0·522714E − 01	−0·138650E + 00	131·79
7	5296·50	4893·33	−2026·88	0·552455E − 01	−0·124911E + 00	126·31
8	5239·59	5138·91	−1022·19	0·552031E − 01	−0·110800E + 00	124·95
9	4902·47	4902·47	0·00	0·515642E − 01	−0·969989E − 01	116·92
10	4356·41	4272·71	849·89	0·448103E − 01	−0·845761E − 01	103·89
11	3291·80	3041·23	1259·72	0·352931E − 01	−0·745146E − 01	78·50
12	1464·93	1218·05	813·87	0·240547E − 01	−0·671060E − 01	34·94
13	0·00	0·00	0·00	0·146115E − 01	−0·609564E − 01	0·00
14	0·00	0·00	0·00	0·903368E − 02	−0·544780E − 01	0·00
15	0·00	0·00	0·00	0·516735E − 02	−0·494817E − 01	0·00
16	0·00	0·00	0·00	0·237886E − 02	−0·464425E − 01	0·00
17	0·00	0·00	0·00	0·000000E + 00	−0·453834E − 01	0·00

TABLE 5

Results for Lug with −0.06 mm Interference Fit Pin; Pin Load of 50,000 N

Iteration 1000 Pin Load		Force N 49970·79	Displacement mm Fit −0·060000			Contact Pressure MPa RPIN 16·865600
POINT	RLOAD	XLOAD	YLOAD	XDISPL	YDISPL	Contact Pressure
1	6021·10	0·00	−6021·10	0·000000E + 00	−0·181929E + 00	143·68
2	5998·58	1170·26	−5883·31	0·154555E − 01	−0·179677E + 00	143·14
3	5925·84	2267·72	−5474·76	0·290436E − 01	−0·174334E + 00	141·40
4	5985·04	3325·11	−4976·38	0·413645E − 01	−0·165777E + 00	142·82
5	5956·26	4211·71	−4211·71	0·513617E − 01	−0·154615E + 00	142·13
6	5917·94	4920·59	−3287·83	0·586868E − 01	−0·141152E + 00	141·22
7	5715·04	5280·00	−2187·05	0·626955E − 01	−0·126629E + 00	136·37
8	5483·11	5377·75	−1069·70	0·632020E − 01	−0·111562E + 00	130·84
9	5144·54	5144·54	0·00	0·602870E − 01	−0·968619E − 01	122·76
10	4673·60	4583·79	911·77	0·542266E − 01	−0·835855E − 01	111·52
11	3977·64	3674·86	1522·18	0·455565E − 01	−0·725851E − 01	94·92
12	3002·19	2496·23	1667·93	0·351860E − 01	−0·641929E − 01	71·64
13	1413·23	999·30	999·30	0·242410E − 01	−0·587390E − 01	33·72
14	0·00	0·00	0·00	0·150348E − 01	−0·550448E − 01	0·00
15	0·00	0·00	0·00	0·888674E − 02	−0·506763E − 01	0·00
16	0·00	0·00	0·00	0·418975E − 02	−0·479142E − 01	0·00
17	0·00	0·00	0·00	0·000000E + 00	−0·469350E − 01	0·00

TABLE 6

Results for Lug with −0.07 mm Interference Fit Pin; Pin Load of 50,000 N

Iteration 1000 Pin Load		Force N 50000·38	Displacement mm Fit −0·070000			Contact Pressure MPa RPIN 16·865600
POINT	RLOAD	XLOAD	YLOAD	XDISPL	YDISPL	Contact Pressure
1	6565·98	0·00	−6565·98	0·000000E + 00	−0·192420E + 00	156·77
2	6673·38	1301·91	−6545·15	0·173351E − 01	−0·190218E + 00	159·34
3	6563·53	2511·76	−6063·91	0·325565E − 01	−0·184392E + 00	156·71
4	6638·24	3688·01	−5519·49	0·464435E − 01	−0·175093E + 00	158·50
5	6591·76	4661·08	−4661·08	0·577916E − 01	−0·162887E + 00	157·39
6	6572·31	5464·68	−3651·38	0·662875E − 01	−0·148170E + 00	156·92
7	6262·52	5785·81	−2396·56	0·710276E − 01	−0·132155E + 00	149·53
8	6010·44	5894·95	−1172·58	0·721243E − 01	−0·115575E + 00	143·51
9	5601·70	5601·70	0·00	0·694712E − 01	−0·993638E − 01	133·75
10	5141·60	5042·81	1003·08	0·635479E − 01	−0·846565E − 01	122·76
11	4576·74	4228·35	1751·44	0·549096E − 01	−0·722841E − 01	109·28
12	3896·10	3239·49	2164·55	0·444356E − 01	−0·625205E − 01	93·03
13	2804·79	1983·29	1983·29	0·331599E − 01	−0·557934E − 01	66·97
14	1477·08	820·62	1228·14	0·225484E − 01	−0·521624E − 01	35·27
15	175·92	67·32	162·53	0·133409E − 01	−0·505072E − 01	4·20
16	0·00	0·00	0·00	0·631135E − 02	−0·486258E − 01	0·00
17	0·00	0·00	0·00	0·000000E + 00	−0·478279E − 01	0·00

TABLE 7

Results for Lug with 0.05 mm Clearance Fit Pin; Pin Load of 25,000 N

Iteration 1000 Pin Load		Force N 24999·93	Displacement mm Fit 0·050000			Contact Pressure MPa RPIN 16·865600
POINT	RLOAD	XLOAD	YLOAD	XDISPL	YDISPL	Contact Pressure
1	3518·04	0·00	−3518·04	0·000000E + 00	−0·115221E + 00	83·40
2	1794·94	350·18	−1760·45	0·244920E − 02	−0·110539E + 00	42·55
3	2152·83	823·85	−1988·96	0·483156E − 02	−0·107225E + 00	51·04
4	2309·94	1283·33	−1920·64	0·605014E − 02	−0·101842E + 00	54·76
5	2853·42	2017·67	−2017·67	0·608913E − 02	−0·955033E − 01	67·65
6	3409·84	2835·17	−1894·40	0·398010E − 02	−0·876050E − 01	80·84
7	2839·97	2623·79	−1086·81	−0·205937E − 02	−0·778619E − 01	67·33
8	369·33	362·24	−72·05	−0·119151E − 01	−0·665439E − 01	8·76
9	0·00	0·00	0·00	−0·166233E − 01	−0·562861E − 01	0·00
10	0·00	0·00	0·00	−0·178891E − 01	−0·470777E − 01	0·00
11	0·00	0·00	0·00	−0·168879E − 01	−0·390933E − 01	0·00
12	0·00	0·00	0·00	−0·145413E − 01	−0·323668E − 01	0·00
13	0·00	0·00	0·00	−0·115898E − 01	−0·268205E − 01	0·00
14	0·00	0·00	0·00	−0·855187E − 02	−0·226320E − 01	0·00
15	0·00	0·00	0·00	−0·560296E − 02	−0·196317E − 01	0·00
16	0·00	0·00	0·00	−0·279262E − 02	−0·178726E − 01	0·00
17	0·00	0·00	0·00	0·000000E + 00	−0·172818E − 01	0·00

TABLE 8

Results for Lug with 0.05 mm Clearance Fit Pin; Pin Load of 100,000 N

Iteration 1000 Pin Load		Force N 99999·96	Displacement mm Fit 0·050000			Contact Pressure MPa RPIN 16·865600
POINT	RLOAD	XLOAD	YLOAD	XDISPL	YDISPL	Contact Pressure
1	12741·30	0·00	−12741·30	0·000000E + 00	−0·406462E + 00	302·06
2	8696·86	1696·67	−8529·75	0·162813E − 01	−0·393659E + 00	206·18
3	8228·91	3149·07	−7602·52	0·307554E − 01	−0·379901E + 00	195·08
4	9403·28	5224·18	−7818·54	0·432513E − 01	−0·362785E + 00	222·93
5	9913·85	7010·15	−7010·15	0·500730E − 01	−0·340242E + 00	235·03
6	11039·08	9178·66	−6132·99	0·512918E − 01	−0·313844E + 00	261·71
7	12007·83	11093·78	−4595·20	0·447475E − 01	−0·285069E + 00	284·67
8	9945·17	9754·07	−1940·21	0·255929E − 01	−0·252747E + 00	235·77
9	2646·11	2646·11	0·00	−0·517943E − 02	−0·219276E + 00	62·73
10	0·00	0·00	0·00	−0·233322E − 01	−0·187810E + 00	0·00
11	0·00	0·00	0·00	−0·291918E − 01	−0·158979E + 00	0·00
12	0·00	0·00	0·00	−0·290248E − 01	−0·134011E + 00	0·00
13	0·00	0·00	0·00	−0·252503E − 01	−0·112991E + 00	0·00
14	0·00	0·00	0·00	−0·197066E − 01	−0·968269E − 01	0·00
15	0·00	0·00	0·00	−0·133916E − 01	−0·851133E − 01	0·00
16	0·00	0·00	0·00	−0·680175E − 02	−0·782005E − 01	0·00
17	0·00	0·00	0·00	0·000000E + 00	−0·758590E − 01	0·00

TABLE 9

Results for Lug with 0.05 mm Clearance Fit Pin; Pin Load of 200,000 N

Iteration 1000 Pin Load		Force N 199999·98	Displacement mm Fit 0·050000			Contact Pressure MPa RPIN 16·865600
POINT	RLOAD	XLOAD	YLOAD	XDISPL	YDISPL	Contact Pressure
1	21064·69	0·00	−21064·69	0·000000E + 00	−0·777575E + 00	499·39
2	18133·72	3537·71	−17785·28	0·382017E − 01	−0·763124E + 00	429·90
3	17422·33	6667·24	−16096·14	0·706785E − 01	−0·740087E + 00	413·04
4	19200·39	10667·16	−15964·54	0·984533E − 01	−0·708678E + 00	455·19
5	20288·69	14346·27	−14346·27	0·115234E + 00	−0·666913E + 00	480·99
6	22034·22	18320·78	−12241·55	0·119850E + 00	−0·616486E + 00	522·37
7	23629·61	21830·91	−9042·66	0·109034E + 00	−0·561106E + 00	560·19
8	20458·22	20065·12	−3991·20	0·747624E − 01	−0·499191E + 00	485·01
9	8307·11	8307·11	0·00	0·175711E − 01	−0·435312E + 00	196·94
10	0·00	0·00	0·00	−0·266420E − 01	−0·375379E + 00	0·00
11	0·00	0·00	0·00	−0·425514E − 01	−0·318979E + 00	0·00
12	0·00	0·00	0·00	−0·460224E − 01	−0·269849E + 00	0·00
13	0·00	0·00	0·00	−0·417789E − 01	−0·228303E + 00	0·00
14	0·00	0·00	0·00	−0·334147E − 01	−0·196229E + 00	0·00
15	0·00	0·00	0·00	−0·230501E − 01	−0·172926E + 00	0·00
16	0·00	0·00	0·00	−0·117948E − 01	−0·159157E + 00	0·00
17	0·00	0·00	0·00	0·000000E + 00	−0·154484E + 00	0·00

TABLE 10

Results for Lug with −0.04 mm Interference Fit Pin; Pin Load of 30,000 N

Iteration 1000 Pin Load		Force N 29999·92		Displacement mm Fit −0·040000		Contact Pressure MPa RPIN 16·865600
POINT	RLOAD	XLOAD	YLOAD	XDISPL	YDISPL	Contact Pressure
1	3818·23	0·00	−3818·23	0·000000E + 00	−0·112970E + 00	91·00
2	3862·12	753·46	−3787·92	0·100158E − 01	−0·111654E + 00	92·05
3	3797·89	1453·39	−3508·79	0·188127E − 01	−0·108261E + 00	90·52
4	3846·51	2137·01	−3198·26	0·268360E − 01	−0·102866E + 00	91·68
5	3825·12	2704·77	−2704·77	0·333778E − 01	−0·957839E − 01	91·17
6	3800·07	3159·64	−2111·21	0·382326E − 01	−0·872227E − 01	90·57
7	3632·28	3355·79	−1390·01	0·409406E − 01	−0·779376E − 01	86·57
8	3488·59	3421·56	−680·59	0·415141E − 01	−0·683248E − 01	83·15
9	3267·48	3267·48	0·00	0·399187E − 01	−0·589372E − 01	77·88
10	2980·72	2923·45	581·51	0·363521E − 01	−0·504340E − 01	71·04
11	2636·31	2435·64	1008·87	0·312189E − 01	−0·433053E − 01	62·83
12	2172·17	1806·09	1206·79	0·249722E − 01	−0·377524E − 01	51·77
13	1464·25	1035·38	1035·38	0·183214E − 01	−0·339838E − 01	34·90
14	550·96	306·10	458·11	0·120910E − 01	−0·320080E − 01	13·13
15	0·00	0·00	0·00	0·710056E − 02	−0·305576E − 01	0·00
16	0·00	0·00	0·00	0·336047E − 02	−0·291291E − 01	0·00
17	0·00	0·00	0·00	0·000000E + 00	−0·286024E − 01	0·00

TABLE 11

Results for Lug with −0.04 mm Interefrence Fit Pin; Pin Load of 100,000 N

Iteration 1000 Pin Load		Force N 100000·18	Displacement mm Fit −0·040000			Contact Pressure MPa RPIN 16·865600
POINT	RLOAD	XLOAD	YLOAD	XDISPL	YDISPL	Contact Pressure
1	11581·15	0·00	−11581·15	0·000000E + 00	−0·368834E + 00	276·03
2	9501·09	1853·57	−9318·53	0·218767E − 01	−0·360506E + 00	226·45
3	9369·66	3585·61	−8656·44	0·412866E − 01	−0·349445E + 00	223·32
4	9672·80	5373·92	−8042·64	0·582928E − 01	−0·333237E + 00	230·54
5	10120·21	7156·07	−7156·07	0·710031E − 01	−0·312962E + 00	241·21
6	10276·99	8545·00	−5709·59	0·778678E − 01	−0·288290E + 00	244·94
7	10543·55	9740·97	−4034·84	0·786310E − 01	−0·261994E + 00	251·30
8	10639·17	10434·74	−2075·60	0·720986E − 01	−0·234386E + 00	253·57
9	9014·97	9014·97	0·00	0·563066E − 01	−0·206907E + 00	214·86
10	4020·09	3942·85	784·28	0·317429E − 01	−0·181990E + 00	95·81
11	0·00	0·00	0·00	0·109836E − 01	−0·159737E + 00	0·00
12	0·00	0·00	0·00	0·163255E − 02	−0·137416E + 00	0·00
13	0·00	0·00	0·00	−0·281825E − 02	−0·118068E + 00	0·00
14	0·00	0·00	0·00	−0·416538E − 02	−0·102821E + 00	0·00
15	0·00	0·00	0·00	−0·366745E − 02	−0·915927E − 01	0·00
16	0·00	0·00	0·00	−0·207703E − 02	−0·849098E − 01	0·00
17	0·00	0·00	0·00	0·000000E + 00	−0·826220E − 01	0·00

TABLE 12

Results for Lug with −0.04 mm Interference Fit Pin; Pin Load of 200,000 N

Iteration 1000 Pin Load		Force N 199998·16	Displacement mm Fit −0·040000			Contact Pressure MPa RPIN 16·865600
POINT	RLOAD	XLOAD	YLOAD	XDISPL	YDISPL	Contact Pressure
1	25660·28	0·00	−25660·28	0·000000E + 00	−0·755844E + 00	611·59
2	18255·59	3561·49	−17904·81	0·402526E − 01	−0·732405E + 00	435·10
3	17945·78	6867·55	−16579·74	0·769820E − 01	−0·708175E + 00	427·72
4	18709·07	10394·20	−15556·02	0·109257E + 00	−0·674566E + 00	445·91
5	20117·17	14224·99	−14224·99	0·133402E + 00	−0·633690E + 00	479·47
6	20326·10	16900·54	−11292·58	0·145069E + 00	−0·583475E + 00	484·45
7	21349·44	19724·31	−8170·08	0·145338E + 00	−0·530605E + 00	508·84
8	21873·13	21452·84	−4267·24	0·130441E + 00	−0·475003E + 00	521·32
9	17570·98	17570·98	0·00	0·944047E − 01	−0·419282E + 00	418·79
10	4231·94	4150·63	825·61	0·389088E − 01	−0·368296E + 00	100·86
11	0·00	0·00	0·00	0·588170E − 02	−0·319583E + 00	0·00
12	0·00	0·00	0·00	−0·894125E − 02	−0·273767E + 00	0·00
13	0·00	0·00	0·00	−0·145994E − 01	−0·234319E + 00	0·00
14	0·00	0·00	0·00	−0·145649E − 01	−0·203399E + 00	0·00
15	0·00	0·00	0·00	−0·112488E − 01	−0·180712E + 00	0·00
16	0·00	0·00	0·00	−0·605811E − 02	−0·167234E + 00	0·00
17	0·00	0·00	0·00	0·000000E + 00	−0·162629E + 00	0·00

TABLE 13

Stresses in Lug with Neat Fit Pin; Pin Load of 50,000 N

Radial Distance (mm)	Radial line through Point 1			Radial line through Point 5			Radial line through Point 9		
	σ_R (MPa)	σ_T (MPa)	σ_{RT} (MPa)	σ_R (MPa)	σ_T (MPa)	σ_{RT} (MPa)	σ_R (MPa)	σ_T (MPa)	σ_{RT} (MPa)
16·86	−107·2	151·3	−3·8	−125·1	159·6	−1·2	−42·8	333·4	− 4·8
17·62	− 94·3	147·2	−0·7	−110·1	157·9	−3·5	−34·6	294·2	− 8·0
18·38	− 86·0	142·9	−1·3	−101·0	154·3	−5·8	−22·0	257·8	−16·0
19·65	− 70·3	141·5	−0·9	− 80·4	151·8	−8·3	−13·6	218·7	−16·2
20·92	− 59·0	139·8	−1·1	− 67·0	146·3	−9·8	− 5·2	183·5	−17·4
22·70	− 42·8	141·4	−1·0	− 46·5	144·0	−9·6	− 4·3	149·9	−12·8
24·48	− 30·3	142·4	−1·0	− 31·6	139·6	−8·8	− 0·8	121·4	−10·3
27·05	− 13·9	146·5	−0·5	− 13·9	140·1	−4·9	− 1·4	84·2	− 4·7
29·59	0·5	151·4	−0·7	0·0	142·6	−1·5	1·4	48·3	− 0·8

TABLE 14

Stresses in Lug with 0.05 mm Clearance Fit Pin; Pin Load of 50,000 N

Radial Distance (mm)	Radial line through Point 1			Radial line through Point 5			Radial line through Point 9		
	σ_R (MPa)	σ_T (MPa)	σ_{RT} (MPa)	σ_R (MPa)	σ_T (MPa)	σ_{RT} (MPa)	σ_R (MPa)	σ_T (MPa)	σ_{RT} (MPa)
16·86	−118·1	98·9	−1·8	−133·9	137·7	− 0·7	−9·0	395·9	−4·7
17·62	−103·3	106·7	−1·7	−117·1	140·9	− 5·0	−0·7	341·0	−1·4
18·38	− 96·5	111·9	−1·6	−109·0	140·9	− 8·2	13·8	289·7	−7·4
19·65	− 78·7	120·4	−1·6	− 86·6	143·0	−13·0	14·4	235·5	−5·2
20·92	− 66·8	126·5	−1·5	− 73·0	140·3	−15·8	19·5	190·0	−7·5
22·70	− 48·2	135·8	−1·4	− 49·9	140·5	−16·0	11·6	146·8	−3·7
24·48	− 34·2	143·8	−1·2	− 33·7	137·6	−14·8	9·7	110·3	−3·1
27·05	− 15·7	156·6	−0·7	− 14·6	140·8	− 8·1	2·6	60·6	−1·2
29·59	0·5	170·0	−0·7	0·1	146·6	− 1·8	1·4	10·7	−0·8

TABLE 15

Stresses in Lug with −0.04 mm Interference Fit Pin; Pin Load of 50,000 N

Radial Distance (mm)	Radial line through Point 1			Radial line through Point 5			Radial line through Point 9		
	σ_R (MPa)	σ_T (MPa)	σ_{RT} (MPa)	σ_R (MPa)	σ_T (MPa)	σ_{RT} (MPa)	σ_R (MPa)	σ_T (MPa)	σ_{RT} (MPa)
16·86	−128·6	211·1	−4·6	−125·2	218·9	−1·7	−114·4	230·8	−1·4
17·62	−110·1	202·1	−1·4	−108·7	208·9	−1·2	−95·9	219·9	−1·5
18·38	− 99·4	191·4	−2·1	− 97·7	197·8	−2·2	−85·9	207·6	−3·4
19·65	− 78·8	181·1	−1·4	− 76·9	185·6	−2·3	−65·0	193·0	−3·9
20·92	− 64·4	170·0	−1·8	− 62·6	172·5	−2·9	−51·1	176·9	−4·4
22·70	− 45·2	161·4	−1·2	− 43·6	161·9	−2·6	−33·8	162·0	−2·7
24·48	− 30·5	152·3	−1·4	− 29·6	150·9	−2·6	−20·4	147·2	−1·8
27·05	− 13·7	146·0	−0·7	− 13·1	142·6	−1·5	− 8·6	135·8	1·7
29·59	0·5	142·2	0·6	0·0	135·6	−1·3	0·8	128·7	3·8

TABLE 16

Stresses in Lug with −0.05 mm Interference Fit Pin; Pin Load of 50,000 N

Radial Distance (mm)	Radial line through Point 1			Radial line through Point 5			Radial line through Point 9		
	σ_R (MPa)	σ_T (MPa)	σ_{RT} (MPa)	σ_R (MPa)	σ_T (MPa)	σ_{RT} (MPa)	σ_R (MPa)	σ_T (MPa)	σ_{RT} (MPa)
16·86	−134·8	232·6	−5·2	−132·5	236·9	−1·8	−116·3	236·7	−1·6
17·62	−115·2	221·3	−1·4	−114·7	225·7	−1·1	−99·0	224·7	0·0
18·38	−103·6	208·1	−2·3	−103·0	213·1	−2·1	−88·1	212·0	−0·4
19·65	− 82·0	195·4	−1·4	− 80·7	199·1	−2·2	−67·5	197·4	0·5
20·92	− 66·9	181·9	−1·9	− 65·5	184·2	−2·7	−53·3	182·2	0·7
22·70	− 46·8	171·1	−1·3	− 45·4	171·7	−2·3	−35·8	169·1	2·5
24·48	− 31·4	159·8	−1·5	− 30·7	158·9	−2·4	−21·7	155·8	3·0
27·05	− 14·1	151·4	−0·7	− 13·5	148·6	−1·4	− 9·2	147·9	5·0
29·59	0·5	145·6	0·7	0·0	139·8	−1·4	0·7	144·7	5·2

TABLE 17

Stresses in Lug with −0.06 mm Interference Fit Pin; Pin Load of 50,000 N

Radial Distance (mm)	Radial line through Point 1			Radial line through Point 5			Radial line through Point 9		
	σ_R (MPa)	σ_T (MPa)	σ_{RT} (MPa)	σ_R (MPa)	σ_T (MPa)	σ_{RT} (MPa)	σ_R (MPa)	σ_T (MPa)	σ_{RT} (MPa)
16·86	−141·8	263·3	−6·0	−143·1	260·0	−2·1	−121·9	252·6	−1·7
17·62	−121·4	248·1	−1·3	−123·9	247·2	−1·1	−104·2	239·3	1·0
18·38	−108·5	231·5	−2·4	−111·1	233·0	−2·2	−92·1	225·3	1·2
19·65	− 85·8	215·3	−1·3	− 87·0	216·9	−2·0	−71·0	209·7	3·1
20·92	− 69·7	198·8	−1·9	−70·5	200·2	−2·5	−55·8	194·1	3·9
22·70	− 48·9	185·3	−1·2	− 48·8	185·8	−2·1	−37·8	181·2	6·0
24·48	− 32·8	171·5	−1·5	− 32·9	171·3	−2·3	−22·9	168·5	6·5
27·05	− 14·7	160·3	−7·5	− 14·5	159·3	−1·4	− 9·7	162·1	7·5
29·59	0·6	152·0	0·7	0·0	148·9	−1·5	0·7	160·9	6·4

TABLE 18

Stresses in Lug with −0.07 mm Interference Fit Pin; Pin Load of 50,000 N

Radial Distance (mm)	Radial line through Point 1			Radial line through Point 5			Radial line through Point 9		
	σ_R (MPa)	σ_T (MPa)	σ_{RT} (MPa)	σ_T (MPa)	σ_T (MPa)	σ_{RT} (MPa)	σ_R (MPa)	σ_T (MPa)	σ_{RT} (MPa)
16·86	−156·0	294·9	−6·8	−158·1	290·4	−2·3	−132·7	279·4	−1·9
17·62	−133·6	277·2	−1·4	−136·8	275·7	−1·2	−113·6	264·2	1·5
18·38	−119·2	258·2	−2·6	−122·5	259·5	−2·4	−100·1	248·5	2·0
19·65	− 94·2	239·5	−1·4	− 95·9	241·2	−2·2	−77·2	230·9	4·6
20·92	− 76·5	220·5	−2·1	− 77·5	222·0	−2·8	−60·5	213·6	5·8
22·70	− 53·5	204·9	−1·3	− 53·7	205·6	−2·3	−41·0	199·6	8·3
24·48	− 35·9	189·0	−1·7	− 36·1	188·9	−2·5	−24·7	185·8	8·9
27·05	− 16·1	175·8	−0·8	− 15·9	174·9	−1·5	−10·5	179·5	9·4
29·59	0·6	166·0	0·8	0·0	162·8	−1·7	0·8	178·9	7·4

TABLE 19

Experimental Strains in Lug for Neat Fit Pin; Pin Load of 50,000 N

Gauge Number	Gauge Location: Distance from centre of Lug hole (mm)	Gauge Location: Angular coordinates degrees	Type of strain measured	Value of strain 10^{-3} m/m
1	18·14	90	Tangential	4·12
2	18·42	45	,,	2·25
3	18·24	0	,,	2·25
4	28·38	90	,,	0·67
5	27·95	45	,,	2·14
6	27·88	0	,,	1·86
7	17·63	90	Radial	−2·48
8	17·77	45	,,	−1·80
9	17·64	0	,,	−1·20

TABLE 20

Theoretical strains in lug for neat Fit Pin; Pin load of 50,000 N

Radial distance (mm)	Radial line through point 1		Radial line through point 5		Radial line through point 9	
	ϵ_R 10^{-3} m/m	ϵ_T 10^{-3} m/m	ϵ_R 10^{-3} m/m	ϵ_T 10^{-3} m/m	ϵ_R 10^{-3} m/m	ϵ_T 10^{-3} m/m
16·86	−2·192	2·614	−2·481	2·811	−2·106	4·888
17·62	−1·992	2·499	−2·262	2·720	−1·813	4·299
18·38	−1·855	2·400	−2·117	2·627	−1·473	3·730
19·65	−1·628	2·310	−1·817	2·500	−1·178	3·142
20·92	−1·463	2·235	−1·604	2·363	−0·900	2·607
22·70	−1·240	2·185	−1·304	2·237	−0·737	2·131
24·48	−1·069	2·142	−1·075	2·108	−0·558	1·713
27·05	−0·856	2·125	−0·827	2·036	−0·399	1·192
29·59	−0·674	2·130	−0·642	2·008	−0·197	0·674

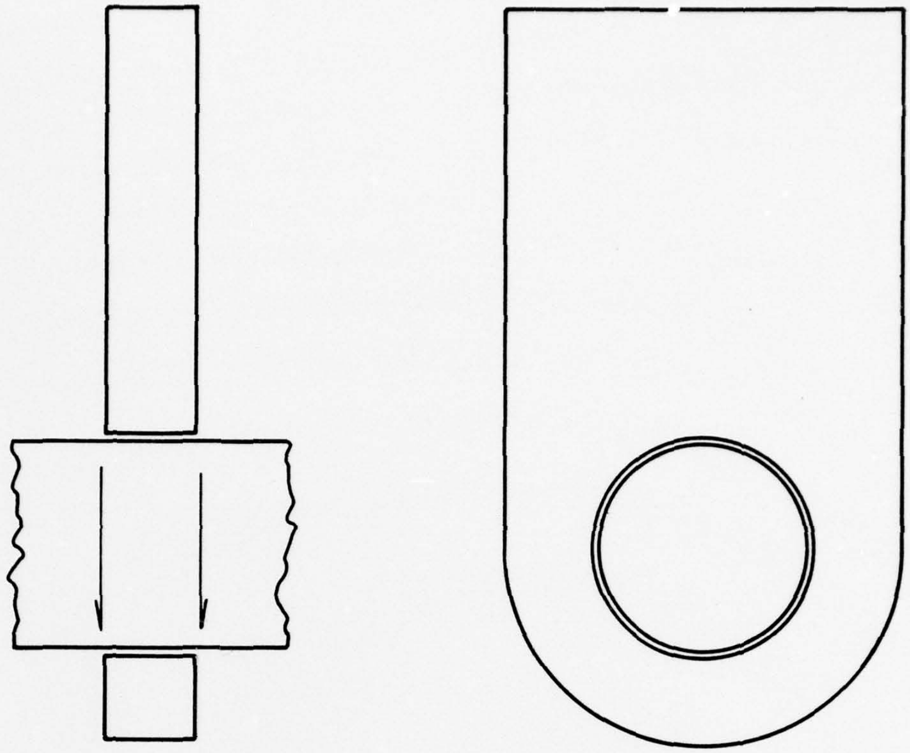

FIG. 1 GEOMETRY OF LUG

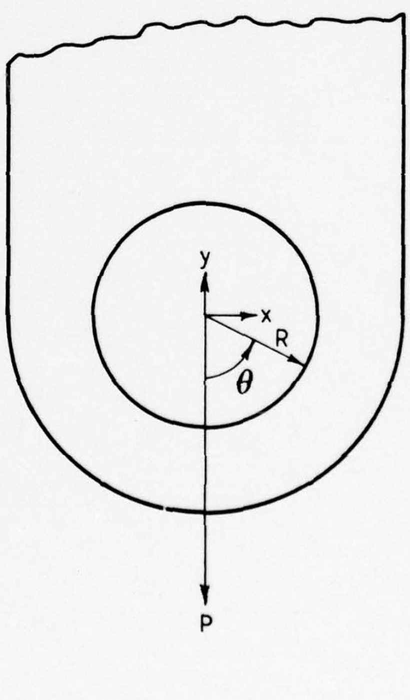

FIG. 2 SIGN CONVENTION

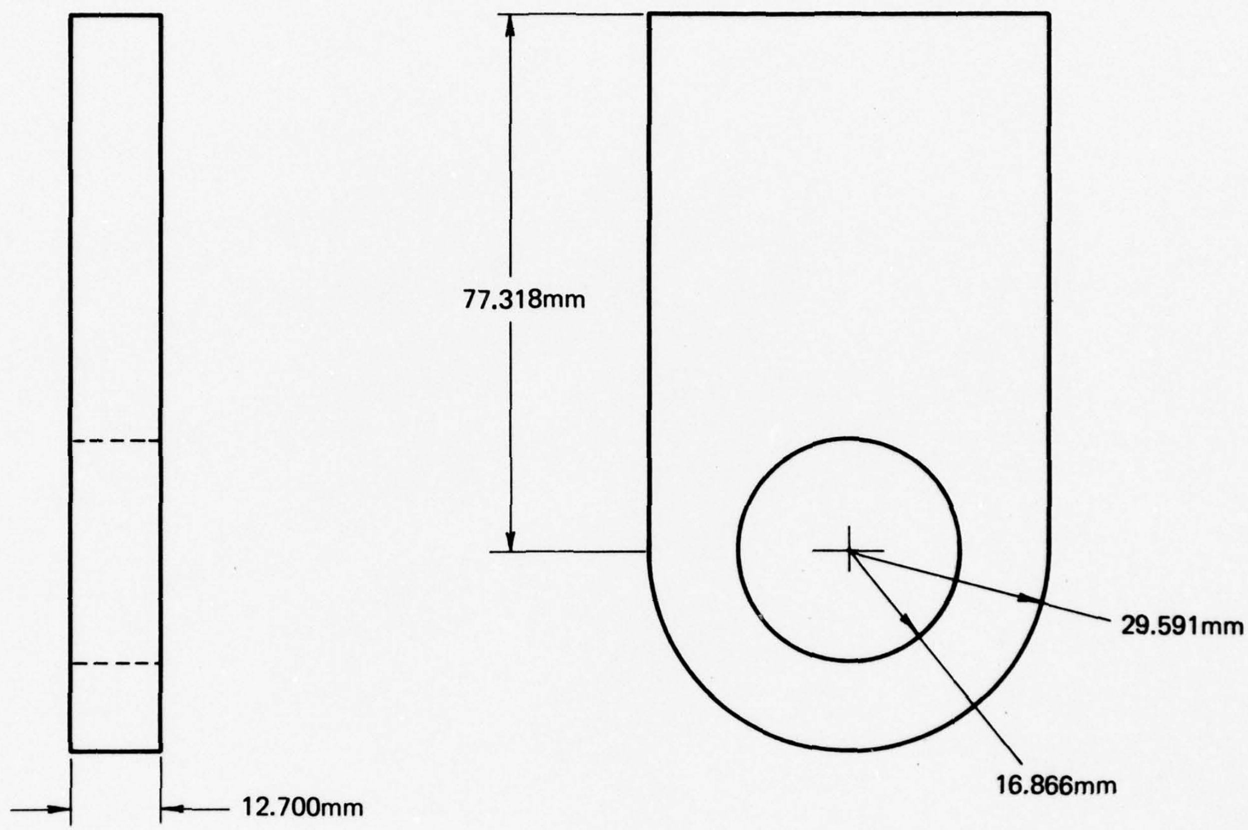

FIG. 3 DIMENSIONS OF LUG

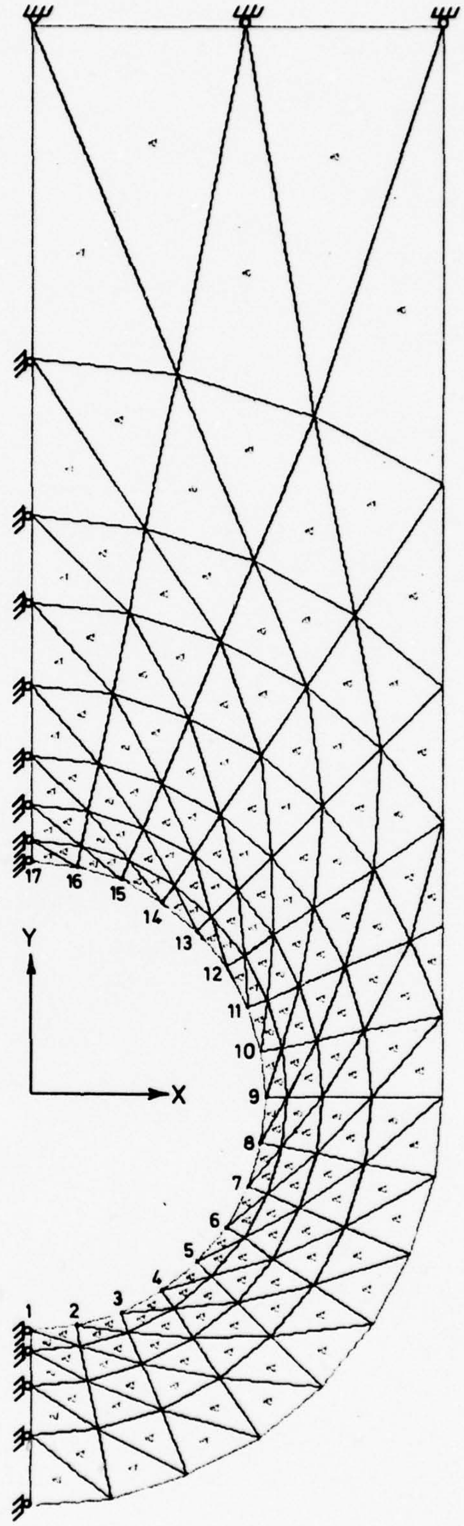

FIG. 4 FINITE ELEMENT IDEALIZATION OF LUG

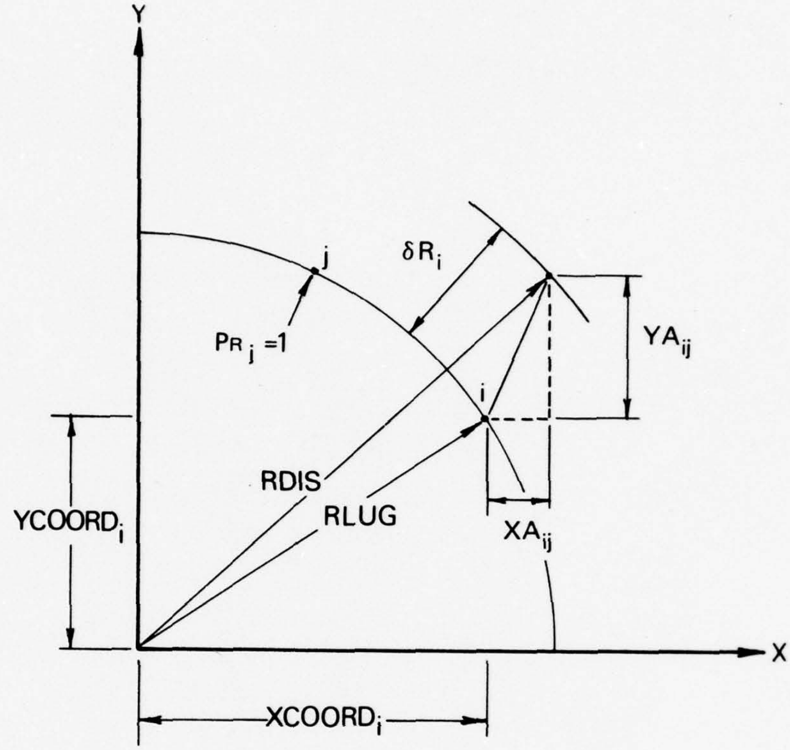

FIG. 5 RADIAL DISPLACEMENT OF POINT i DUE TO UNIT RADIAL LOAD AT j

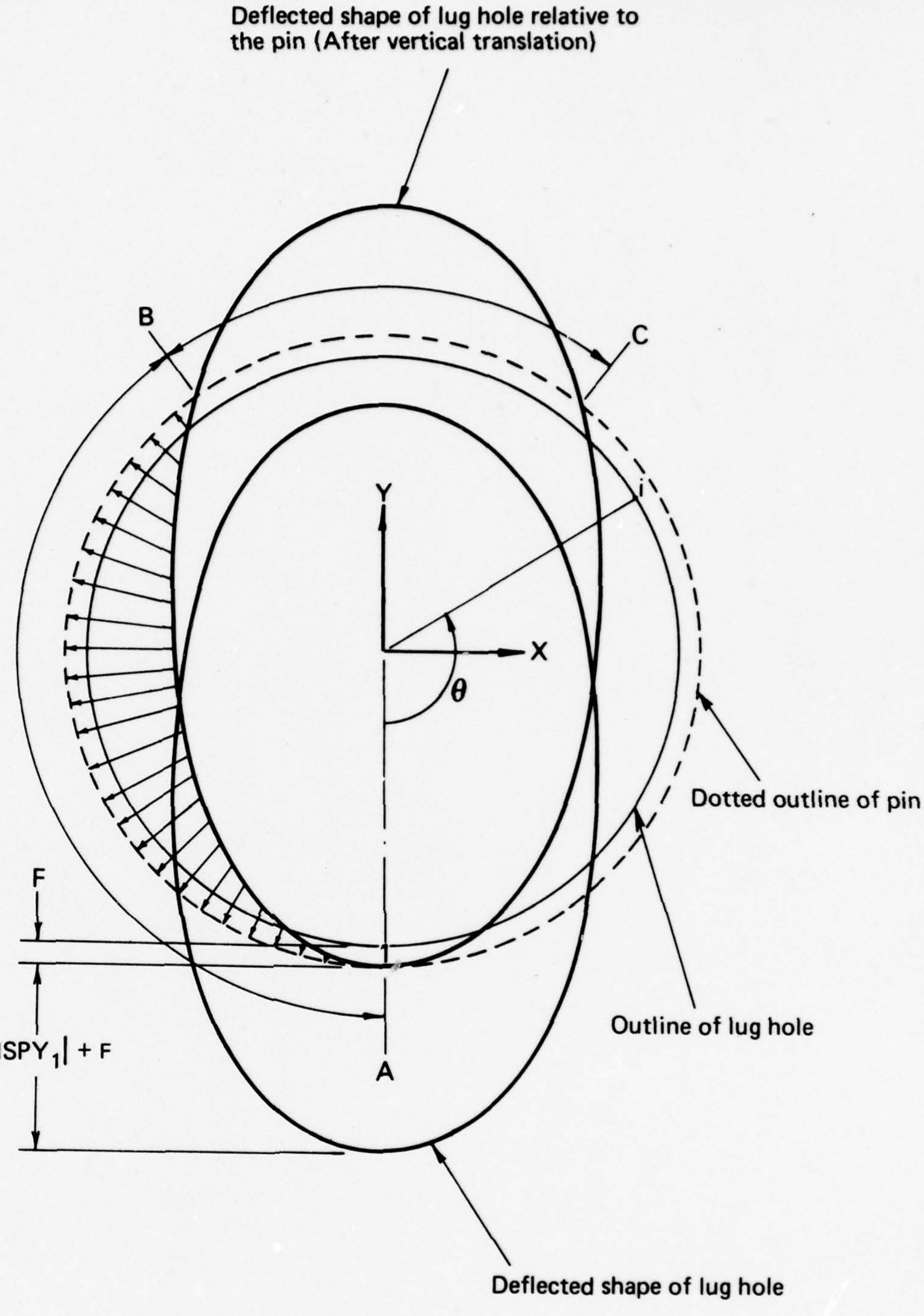

FIG. 6 GEOMETRY OF PIN AND LUG

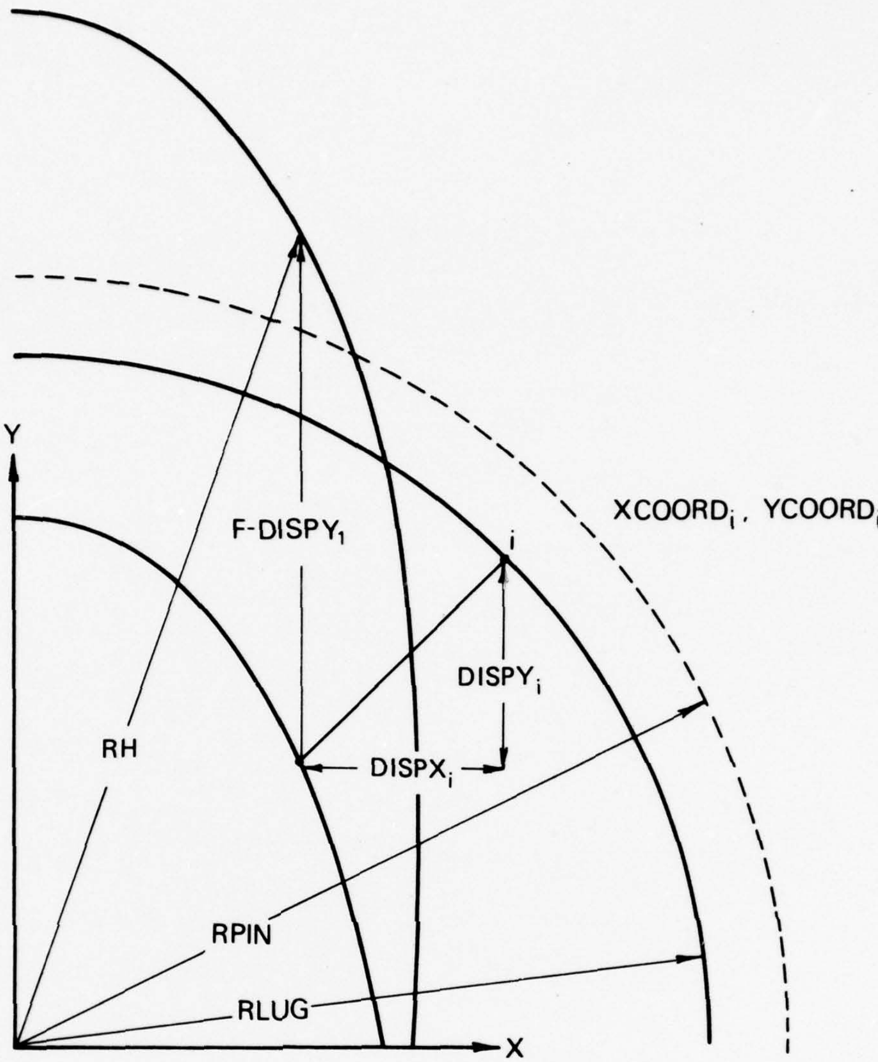

FIG. 7 DISPLACEMENT OF POINT i RELATIVE TO THE CENTRE OF THE PIN

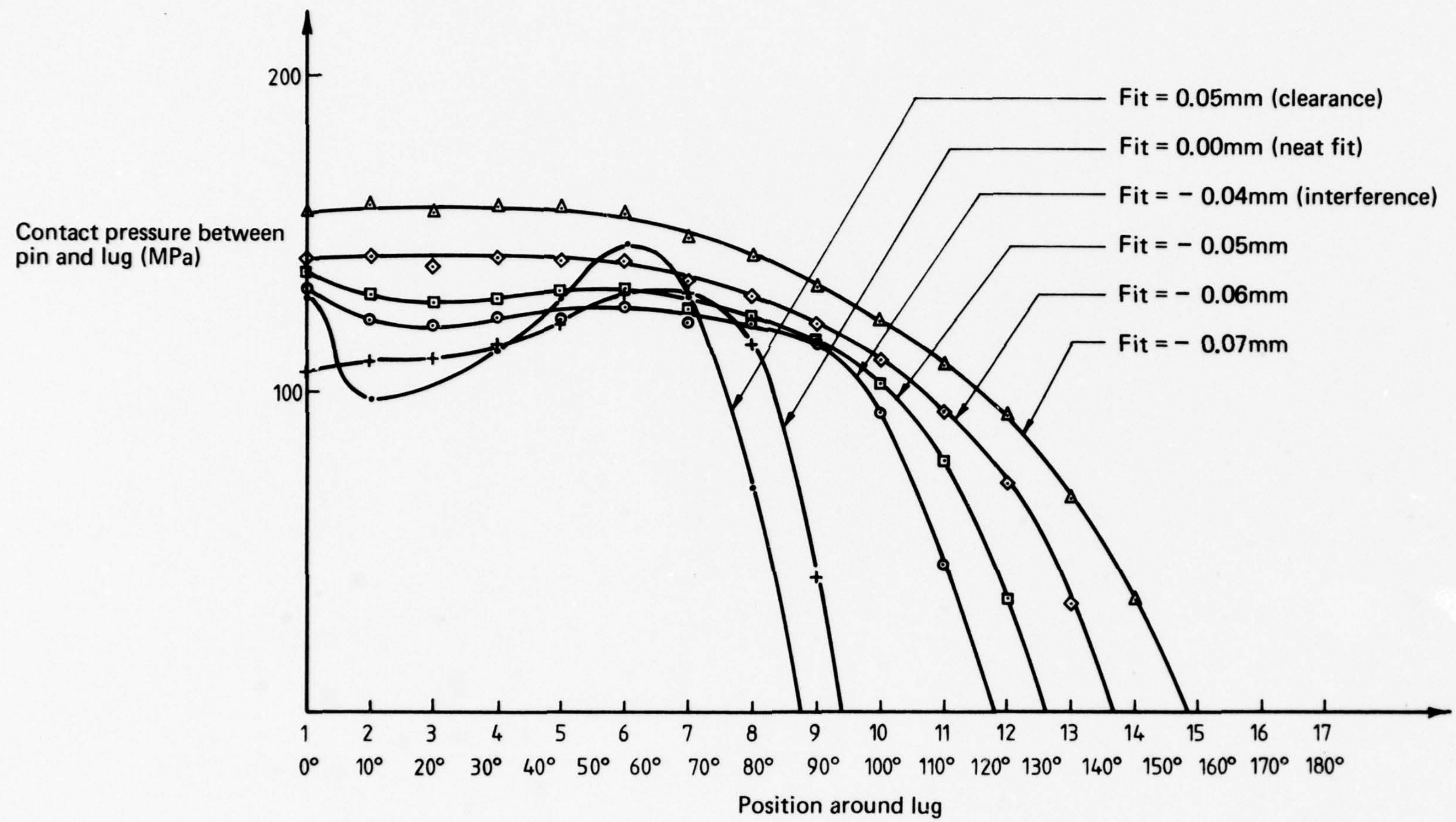

FIG. 8 LOAD DISTRIBUTIONS FOR VARIOUS FITS ; PIN LOAD IS 50kN

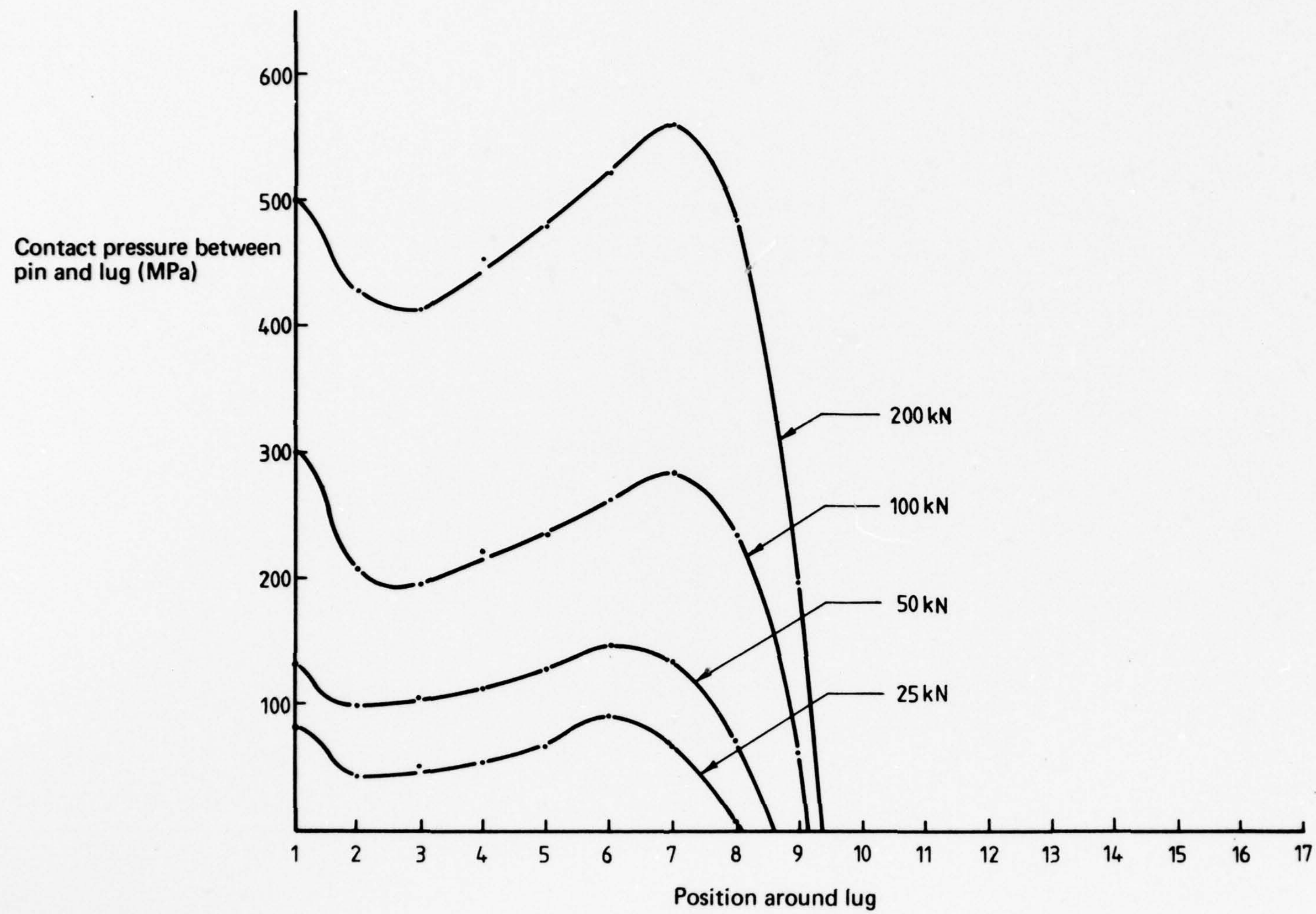

FIG. 9 LOAD DISTRIBUTIONS FOR A CLEARANCE FIT OF 0.05mm

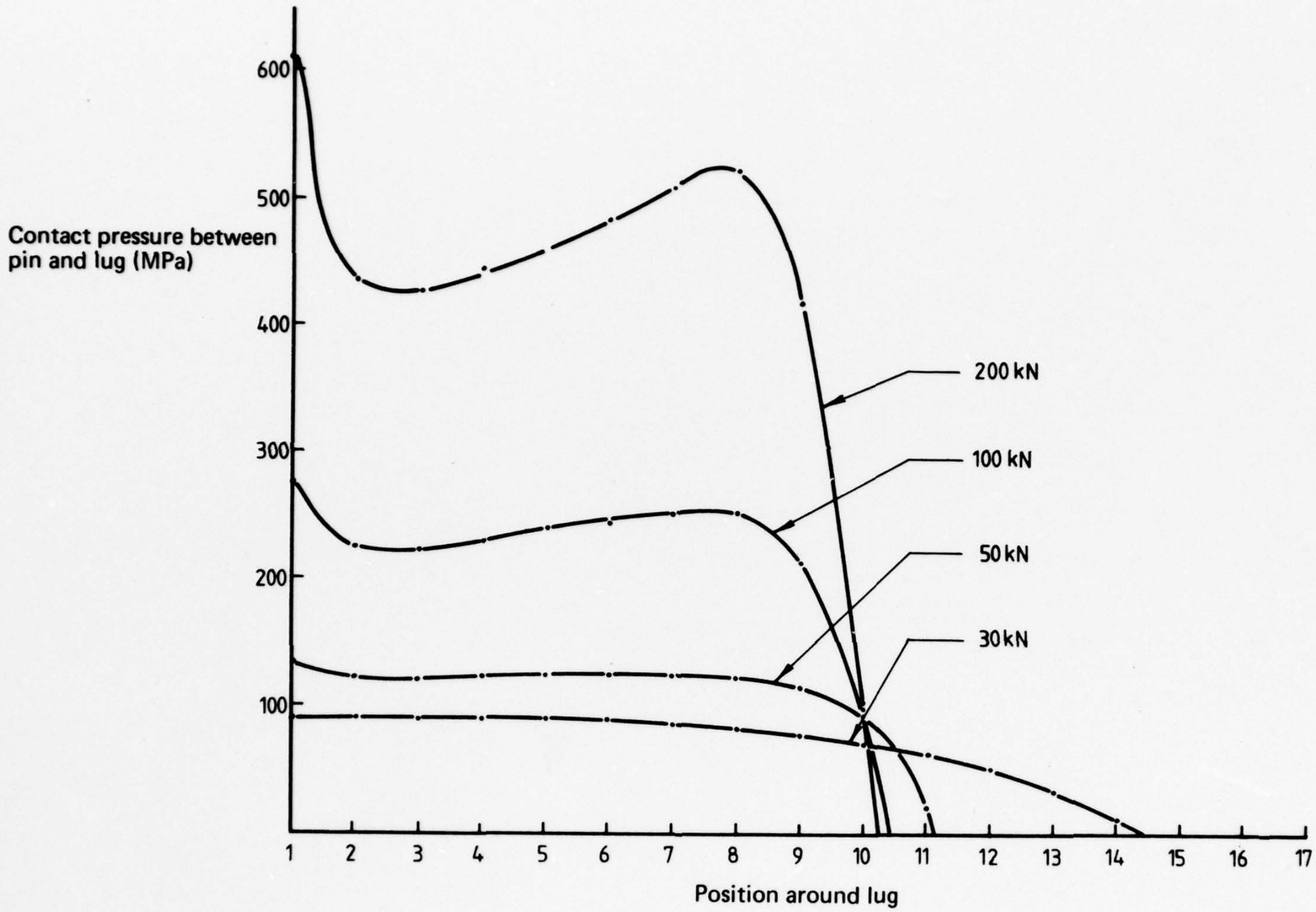

FIG. 10 LOAD DISTRIBUTIONS AROUND LUG FOR AN INTERFERENCE FIT OF − 0.04mm

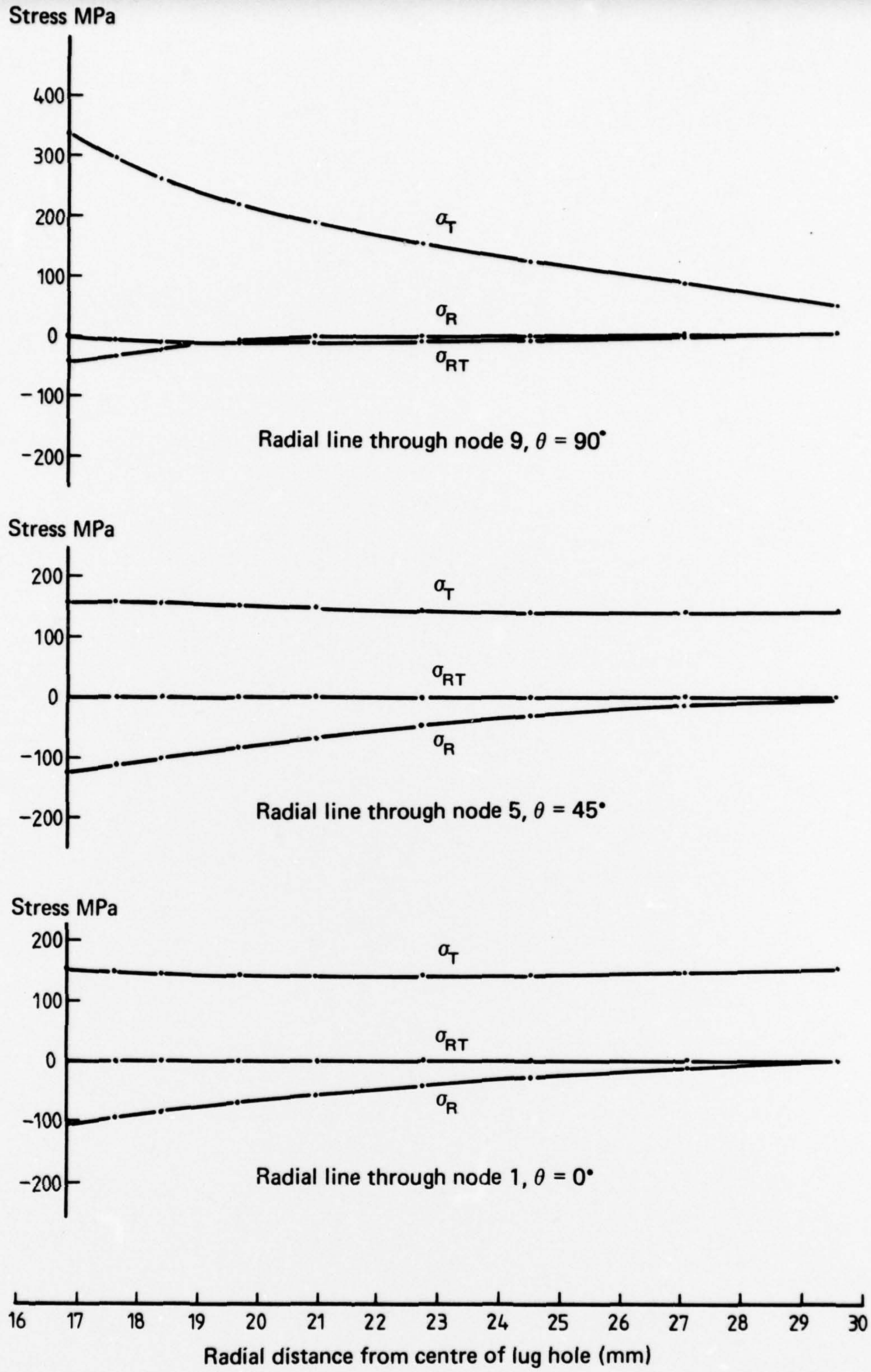

FIG. 11 THEORETICAL STRESSES FOR A NEAT FIT ; PIN LOAD IS 50kN

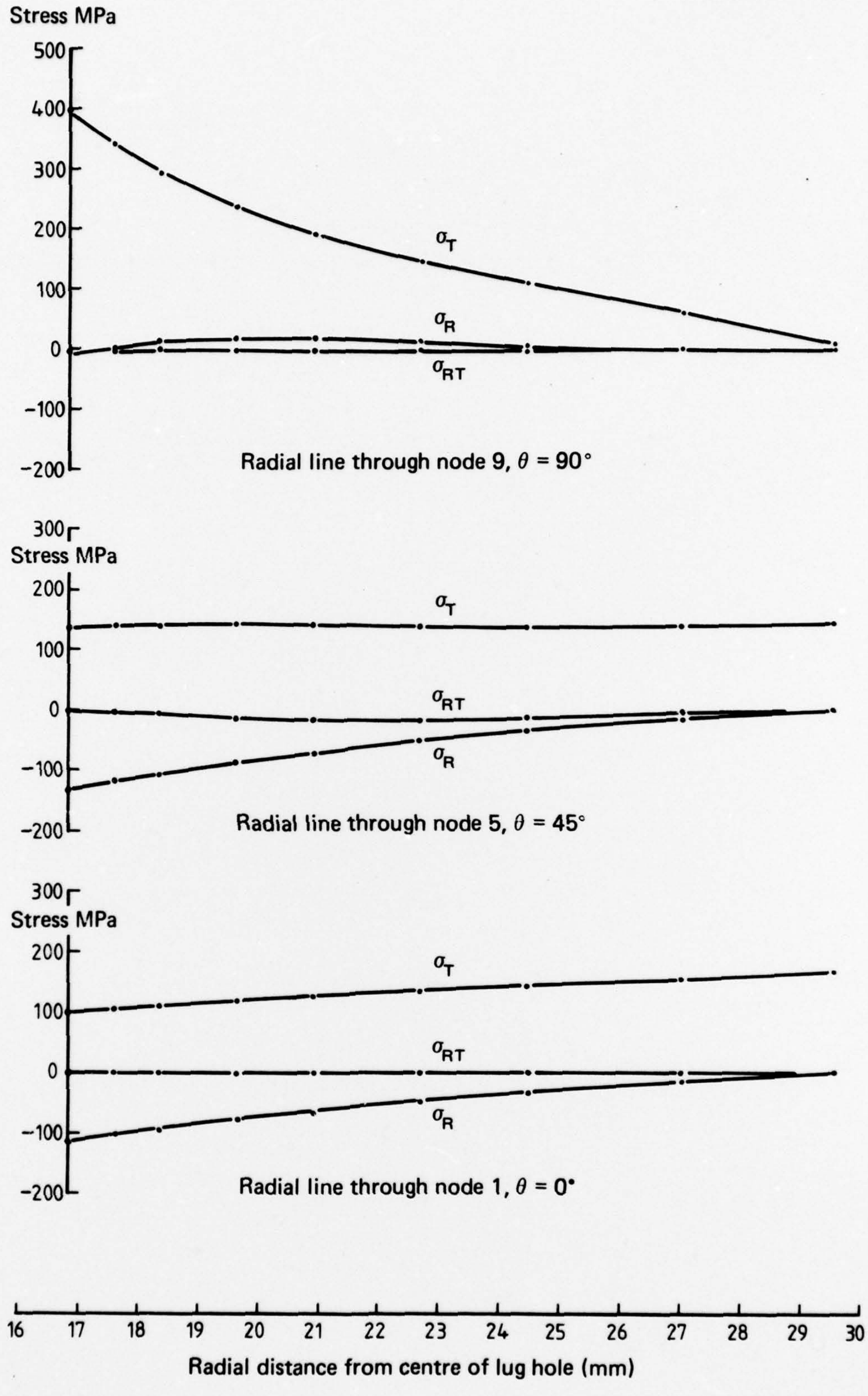

FIG. 12 THEORETICAL STRESSES FOR A CLEARANCE FIT OF 0.05mm ;
PIN LOAD IS 50kN

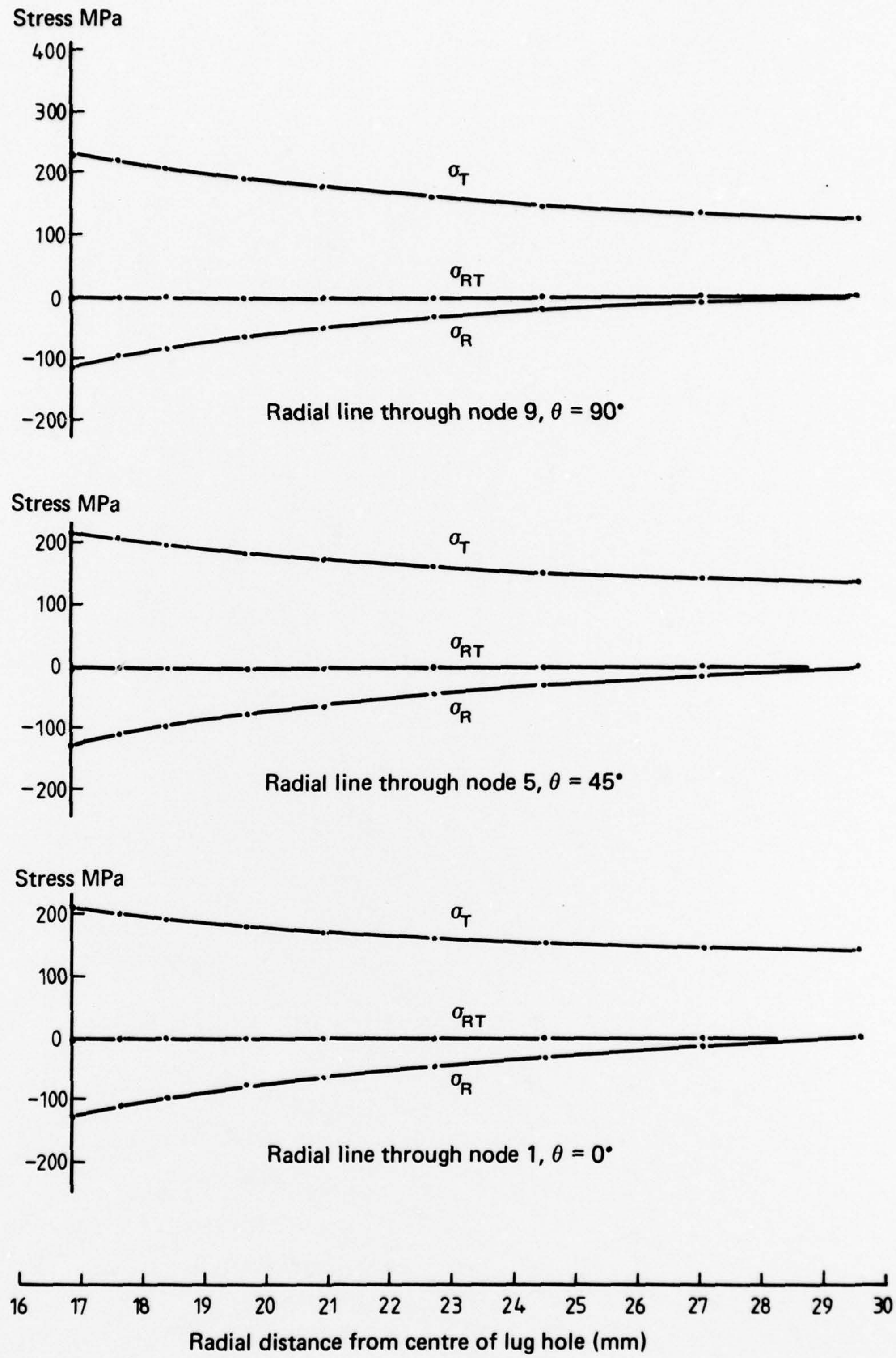

FIG. 13 THEORETICAL STRESSES FOR AN INTERFERENCE OF −0.04mm ; PIN LOAD IS 50kN

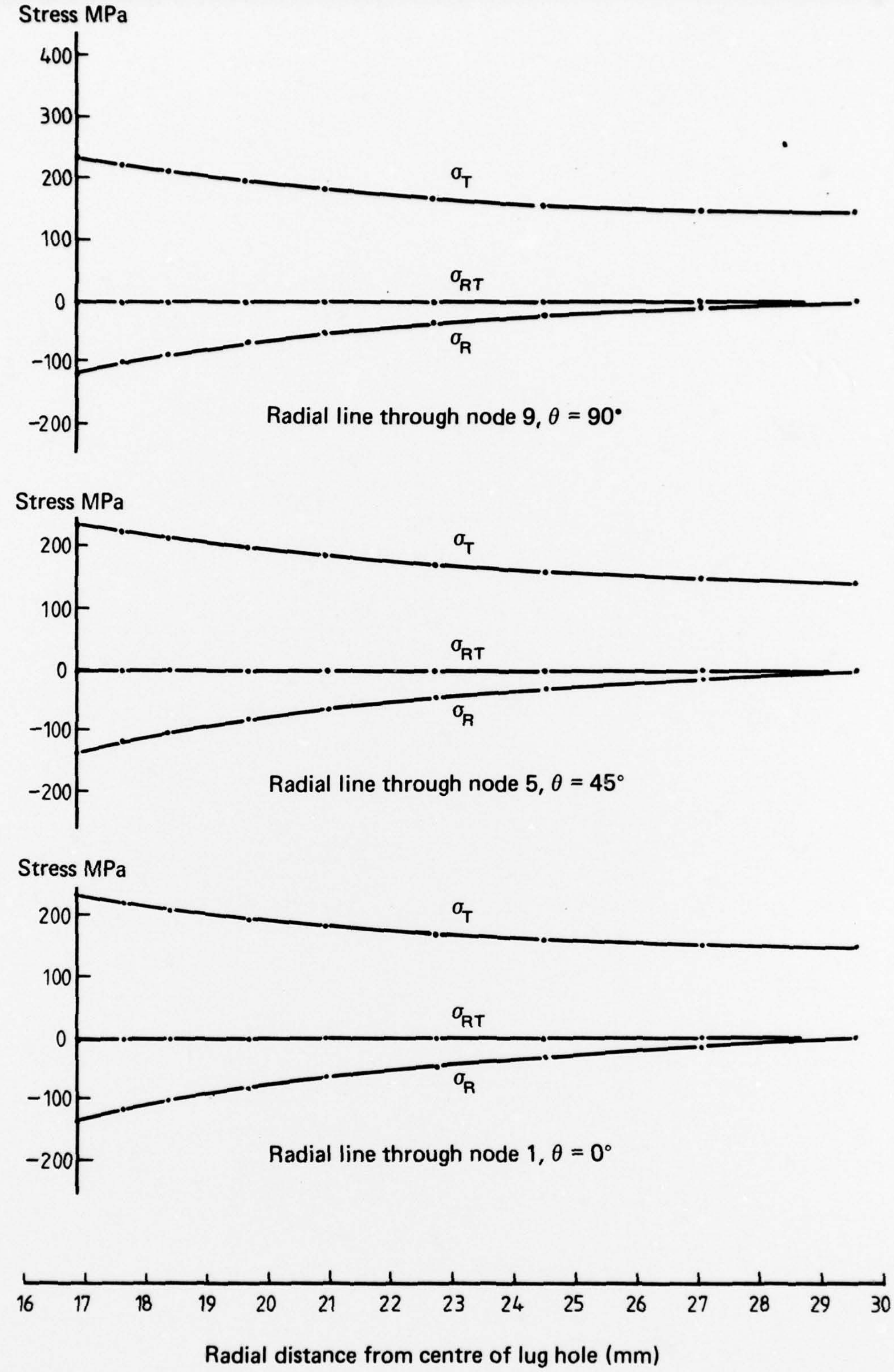

FIG. 14 THEORETICAL STRESSES FOR AN INTERFERENCE OF −0.05mm ; PIN LOAD IS 50kN

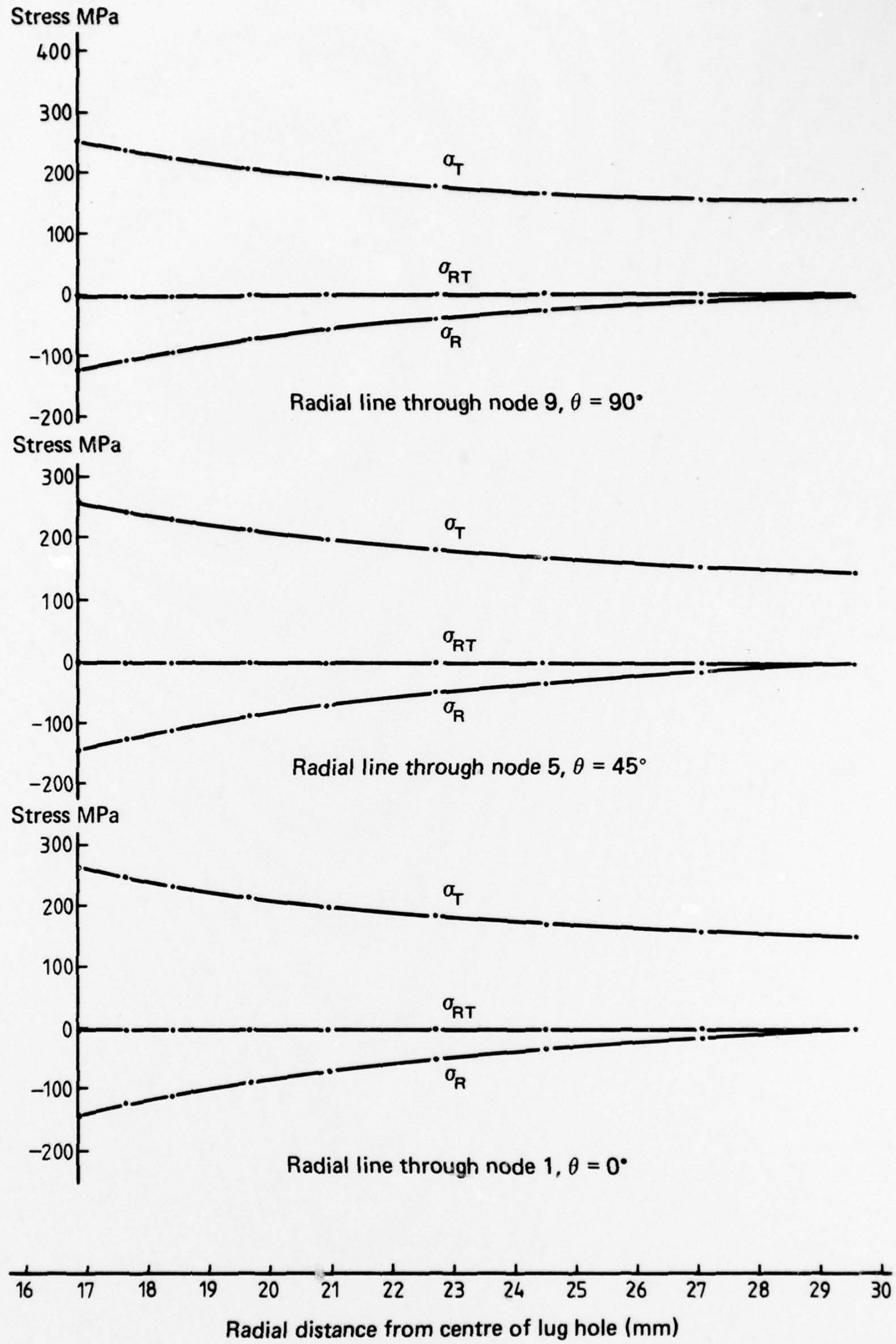

FIG. 15 THEORETICAL STRESSES FOR AN INTERFERENCE OF – 0.06mm ; PIN LOAD IS 50kN

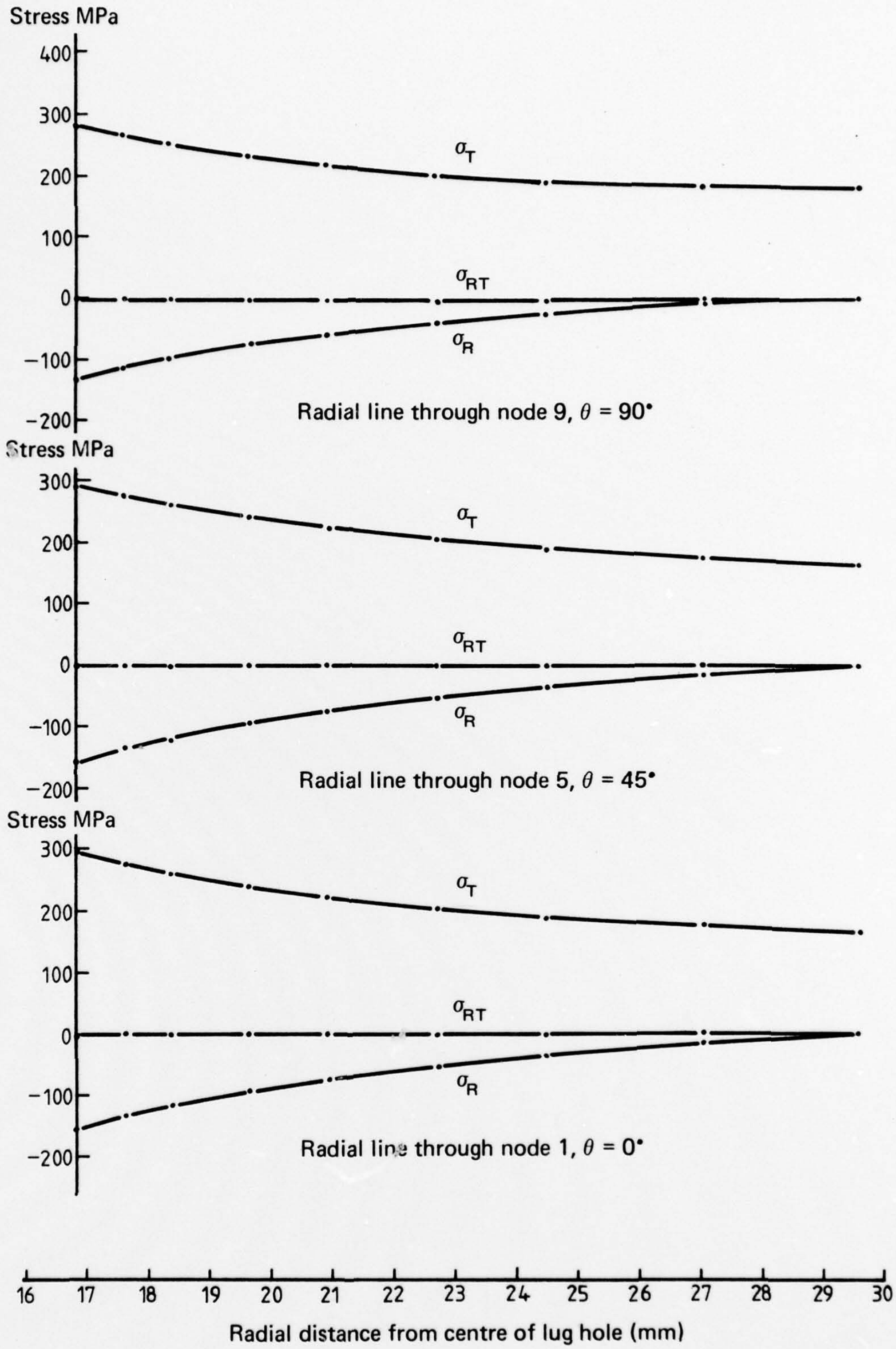

FIG. 16 THEORETICAL STRESSES FOR AN INTERFERENCE OF − 0.07mm ; PIN LOAD IS 50kN

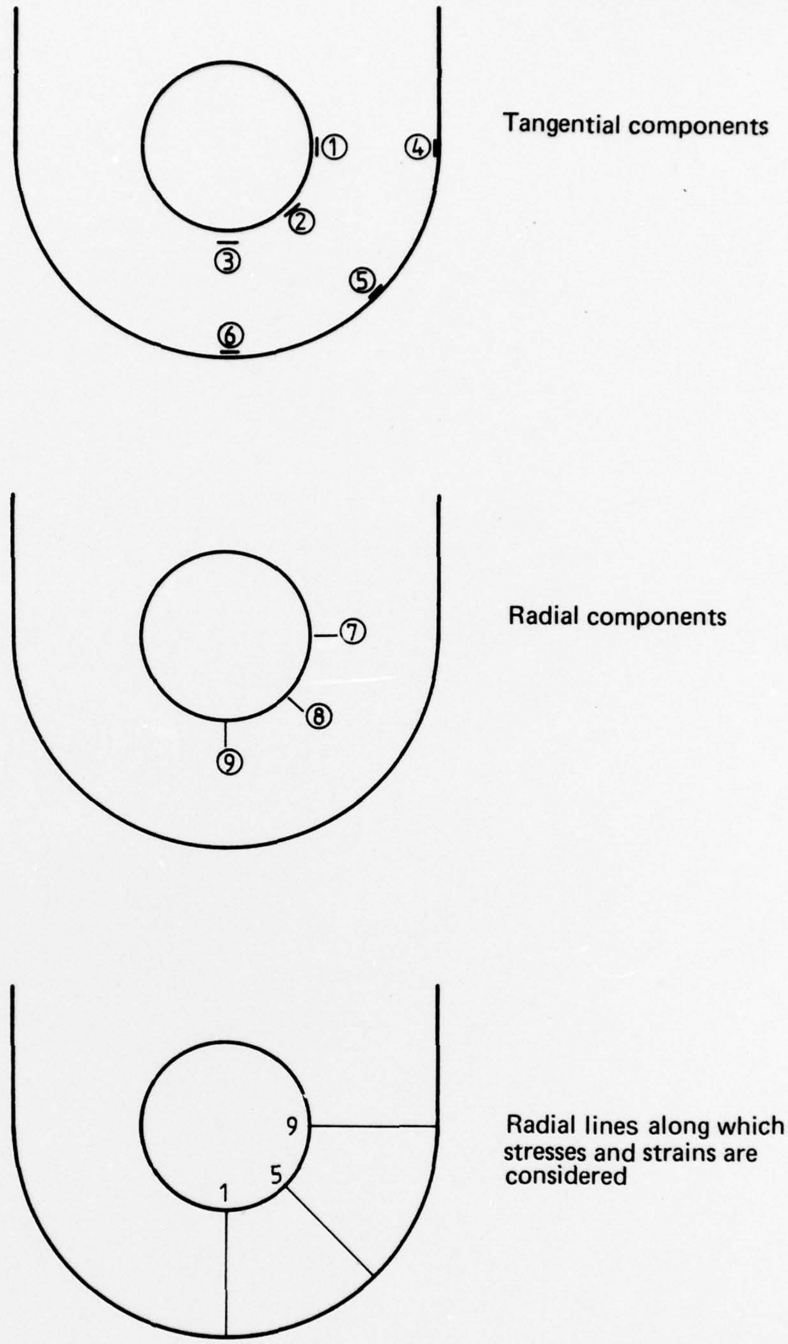

FIG. 17 POSITION OF STRAIN GAUGES

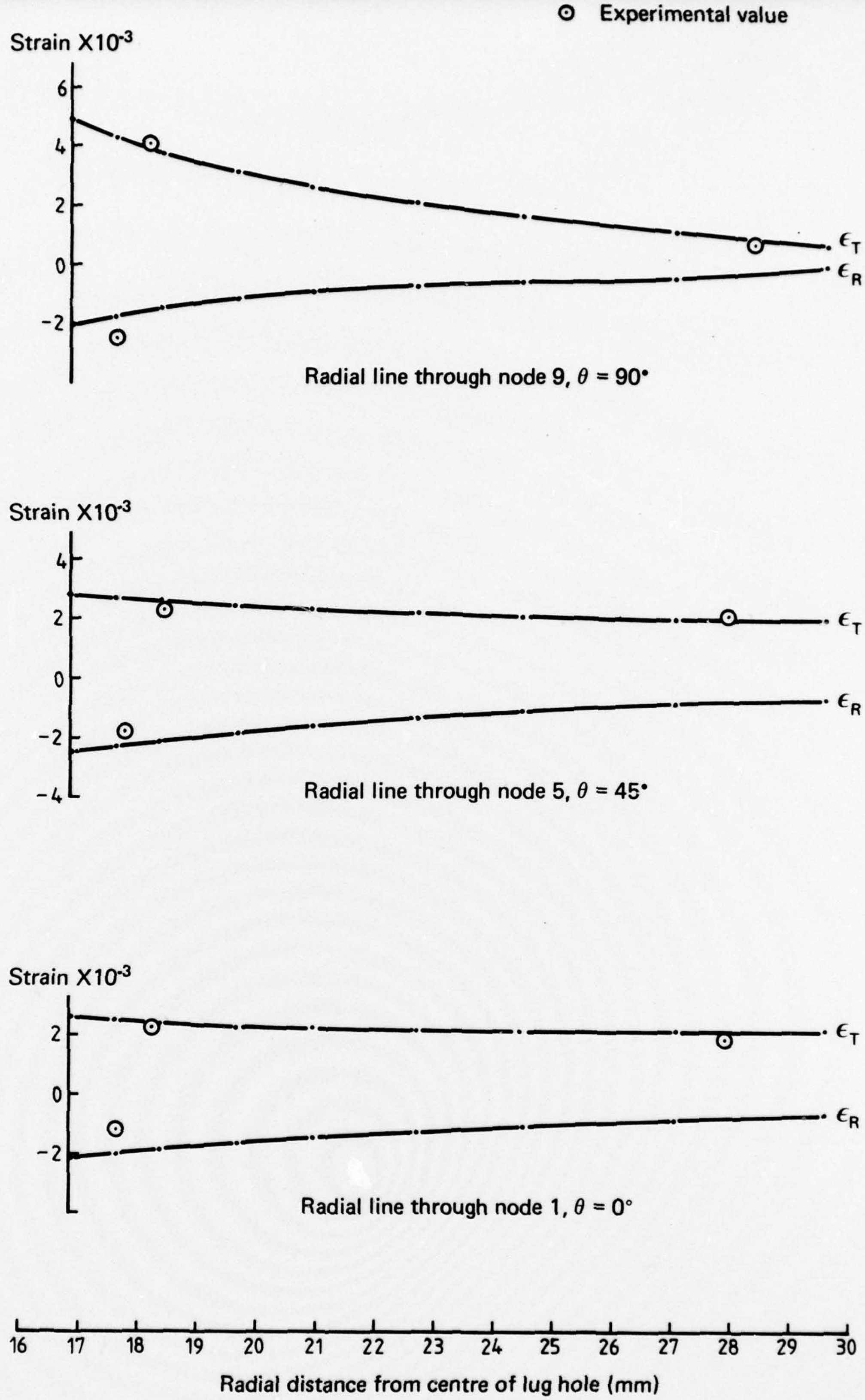

FIG. 18 THEORETICAL AND EXPERIMENTAL STRAINS FOR A NEAT FIT

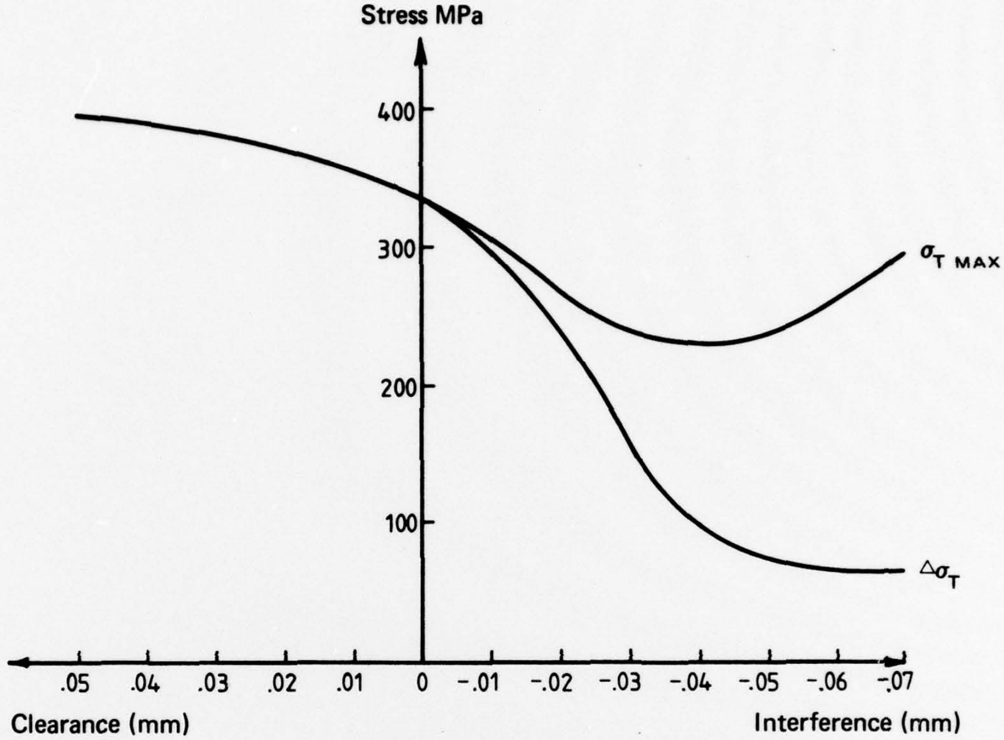

FIG. 19 VARIATION OF TANGENTIAL STRESS AND INCREMENT OF TANGENTIAL STRESS WITH FIT

DISTRIBUTION

AUSTRALIA

DEPARTMENT OF DEFENCE

Central Office	Copy No.
Chief Defence Scientist	1
Executive Controller, ADSS	2
Superintendent, Defence Science Administration	3
Defence Library	4
J.I.O.	5
Assistant Secretary, DISB	6–22
Aeronautical Research Laboratories	
Chief Superintendent	23
Superintendent — Structures	24
Divisional File — Structures	2
Author — R. J. Callinan	26
B. C. Hoskin	27
R. Carey	28
P. H. Townshend	29
C. A. Patching	30
J. Y. Mann	31
R. A. Bruton	32
A. O. Payne	33
G. S. Jost	34
Library	35
Materials Research Laboratories	
Library	36
Weapons Research Laboratories	
Library	37
Air Office	
Air Force Scientific Adviser	38
Library, Engineering, CAFTS Branch	39
SENGSO, Support Command, H.Q.	40
Library, A.R.D.U. Edinburgh, Sth. Aust.	41
Army Office	
Army Scientific Adviser	42
Library, Engineering Development Est.	43
The Bridges Library, Royal Military College	44
US Army Standardisation Group	45
Navy Office	
Naval Scientific Adviser	46

DEPARTMENT OF PRODUCTIVITY

Government Aircraft Factories, Library	47

AUSTRALIA (continued)

		Copy No.
DEPARTMENT OF NATIONAL RESOURCES		
Secretary, Canberra		48
DEPARTMENT OF TRANSPORT		
Library		49
Airworthiness Group (Mr. R. Ferrari)		50
STATUTORY AND STATE AUTHORITY AND INDUSTRY		
C.S.I.R.O. Central Library		51
C.S.I.R.O., Mechanical Engineering Division (Chief)		52
Qantas, Library		53
Trans Australia Airlines, Library		54
Ansett Airlines of Australia, Library		55
Commonwealth Aircraft Corporation (Manager)		56
Commonwealth Aircraft Corporation (Manager of Engineering)		57
Hawker de Havilland Pty Ltd (Librarian) Bankstown		58
Hawker de Havilland Pty Ltd (Manager) Lidcombe		59
UNIVERSITIES AND COLLEGES		
Adelaide	Barr Smith Library	60
	Professor of Mechanical Engineering	61
Australian National	Library	62
Flinders	Library	63
James Cook	Library	64
La Trobe	Library	65
Melbourne	Engineering Library	66
Monash	Library	67
Newcastle	Library	68
New England	Library	69
New South Wales	Physical Sciences Library	70
Queensland	Library	71
Sydney	Professor G. A. Bird, Aeronautical Engineering	72
Tasmania	Engineering Library	73
Western Australia	Library	74
RMIT	Library	75

CANADA

CAARC Co-ordinator Structures	76
NRC, National Aeronautics Establishment, Library	77
NRC, Division of Mechanical Engineering (Dr D. McPhail, Director)	78
UNIVERSITIES	
McGill Library	79
Toronto Institute of Aerophysics	80

FRANCE

AGARD, Library	81
ONERA, Library	82
Service de Documentation, Technique de l'Aeronautique	83

GERMANY

ZLDI	84

		Copy No.
INDIA		
CAARC Co-ordinator Structures		85–86
Civil Aviation Department (Director)		87
Defence Ministry, Aero Development Establishment, Library		88
Hindustan Aeronautics Ltd, Library		89
Indian Institute of Science, Library		90
Indian Institute of Technology, Library		91
National Aeronautical Laboratory (Director)		92
ISRAEL		
Technion—Israel Institute of Technology (Professor J. Singer)		93
ITALY		
Associazione Italiana di Aeronautica and Astronautica (Professor A. Evla)		94
JAPAN		
National Aerospace Laboratory, Library		95
UNIVERSITIES		
Tohuku (Sendai)	Library	96
Tokyo	Institute of Space and Aerospace	97
NETHERLANDS		
Central Organization for Applied Science Research in the Netherlands TNO, Library		98
National Aerospace Laboratory (NLR), Library		99
NEW ZEALAND		
Air Department, R.N.Z.A.F. Aero Documents Section		100
Transport Ministry, Civil Aviation Division, Library		101
UNIVERSITIES		
Canterbury	Library	102
SWEDEN		
Aeronautical Research Institute		103
Chalmers Institute of Technology, Library		104
SAAB, Library		105
UNITED KINGDOM		
Australasian Defence Selence and Technical Representative		106
Aeronautical Research Council, N.P.L. (Secretary)		107
C.A.A.R.C. N.P.L. (Secretary)		108
Royal Aircraft Establishment Library, Farnborough		109
Royal Aircraft Establishment Library, Bedford		110
Royal Armament Research and Development Establishment, Library		111
Admiralty Materials Laboratories (Dr R. G. Watson)		112
National Engineering Laboratories (Superintendent)		113
British Library, Science Reference Library		114
British Library, Lending Division		115
Naval Construction Research Establishment (Superintendent)		116
C.A.A.R.C. Co-ordinator, Structures		117
Aircraft Research Association, Library		118
British Ship Research Association		119

		Copy No.
AIRCRAFT COMPANIES		
Hawker Siddeley Aviation Ltd, Brough		120
Hawker Siddeley Aviation Ltd, Greengate		121
Hawker Siddeley Aviation Ltd, Kingston-upon-Thames		122
British Aircraft Corporation (Holdings) Ltd, Commercial Aircraft Division		123
British Aircraft Corporation (Holdings) Ltd, Military Aircraft		124
British Aircraft Corporation (Holdings) Ltd, Commercial Aviation Division		125
British Hovercraft Corporation Ltd (E. Cowes)		126
Short Brothers & Harland		127
Westerland Helicopters Ltd		128
UNIVERSITIES AND COLLEGES		
Bristol	Library, Engineering Department	129
Cambridge	Library, Engineering Department	130
Nottingham	Library	131
Southampton	Library	132
Strathclyde	Library	133
Cranfield Institute of Technology	Library	134
Imperial College	The Head	—
UNITED STATE OF AMERICA		
Counsellor, Defence Science		135
N.A.S.A. Scientific and Technical Information Facility		136
American Institute of Aeronautics and Astronautics		137
The John Crerar Library		138
Boeing Co. Head Office		—
Boeing Co. Industrial Production Division		140
Cessna Aircraft Co. (Mr D. W. Mallonee, Executive Engineer) (Structures only)		141
Lockheed Aircraft Co. (Director)		142
McDonnell Douglas Corporation (Director)		143
Battelle Memorial Institute, Library		144
UNIVERSITIES AND COLLEGES		
Cornell (New York)	Library, Aeronautical Laboratories	145
Stanford	Library, Department of Aeronautics	146
Wisconsin	Memorial Library, Serials Department	147
Brooklyn	Library, Polytech Aeronautical Laboratories	148
California	Library, Guggenhein Aeronautical Laboratories	149
International Committee on Aeronautical Fatigue		150–173
Spares		174–185